Hiroshima University Doctoral Thesis

Dynamic Solvent Effect on the Lifetime of Singlet Diradicals with π-Single Bonding

(π 単結合性をもつ一重項ジラジカルの
寿命に及ぼす動的溶媒効果)

2022

Department of Chemistry,

Graduate School of Science,

Hiroshima University

LIU QIAN

Table of Contents

1. Main Thesis

    Dynamic Solvent Effect on the Lifetime of Singlet Diradicals with π-Single Bonding

    (π 単結合性をもつ一重項ジラジカルの寿命に及ぼす動的溶

    媒効果)

2. Articles

Main Thesis

Contents

Chapter 1.
General Introduction

1.1 The study of diradicals

Diradicals, as described by Salem and Rowland, have two odd electrons in degenerate or nearly-degenerate molecular orbitals[1] and owe to their unique electronic structures, diradicals have attracted considerable interest as potential candidates for the construction of functional materials such as organic semiconductors,[2–4] memory materials,[5] non-linear optics[6] and biomaterials.[7]

Diradicals could be categorized into localized and delocalized ones generally. Delocalized diradicals include Kekulé and non-Kekulé types and antiaromatic molecules were also recognized as delocalized diradicals. Typical examples of delocalized diradicals are paraphenylene (PP) and trimethylenemethane (TMM) and they have been broadly investigated since last century on account of the stability of π-conjugation.[8–10] Localized diradicals such as cyclopropane-1,3-diyl diradical (1,3-**DR**), which were first proposed by Chambers and Kistiakowsky,[11] are key intermediates in bond-homolysis processes (Figure 1.1). Therefore, the studies of localized diradicals play a vital role in understanding the nature of chemical bonds including bond-forming and bond-breaking processes.
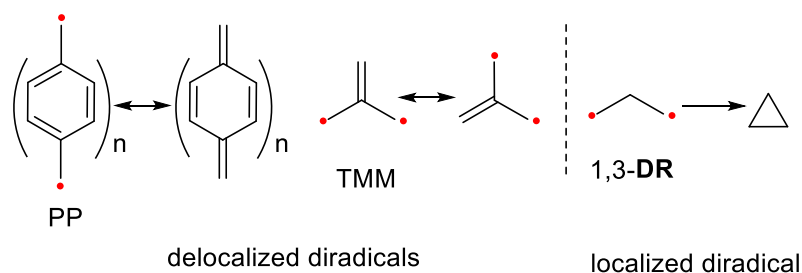

Figure 1.1. The examples of delocalized diradicals and localized diradicals.

As one of the most fundamental properties of localized diradicals, electronic spin state which determined the structure and reactivity have been investigated thoroughly. Based on the Hund's rule,[12] diradicals prefer the triplet ground-state spin multiplicity where the two unpaired

electrons singly occupying two orbitals to avoid electron-electron repulsion. The singlet-triplet energy gap (ΔE_{ST}) which can be obtained according to the electron exchange interaction (J), $\Delta E_{ST} = E_S - E_T = 2J$, provides valuable insight into the spin multiplicity of diradicals. Specifically, a positive ΔE_{ST} indicates triplet ground-state whereas the negative value indicates singlet ground-state. It is noteworthy that the ΔE_{ST} is affected strongly by the substituents. In 2003, Zhang and Borden *et al.* performed unrestricted density functional theory (UDFT) calculations on monocyclic diradicals **DR1−2** to explore *para* substituents effects for the value of ΔE_{ST} (Figure 1.2).[13] They noted that singlet ground-state was computed for **DR1** despite of the π-electron-donating and π-electron-withdrawing *para* substituents. However, comparing with π-electron-withdrawing groups, the π-electron-donating substituents will result in stabilization of singlet diradicals in which case the negative ΔE_{ST} value is larger. Conversely, different from the C−F hyperconjugative interactions in **DR1**, the triplet ground state and negligible substituent effects were obtained for hydrocarbon diradicals **DR2** caused by C−H hyperconjugative interactions. So far, the remarkable substituent effects at C2 position on ground state of localized diradicals has been revealed unambiguously and there are two factors determining the spin multiplicity and the ΔE_{ST} value of diradicals. One is the energy gap between the two electrons occupying two nonbonding molecular orbitals (NBMOs, Ψ_A the lowest unoccupied molecular orbital (LUMO) and Ψ_S the highest occupied molecular orbital (HOMO)) determined by the through-space (TS) and through-bond (TB) interactions. Another one is the exchange repulsion energy (Figure 1.3).[14] A number of experimental and computational work[15−20] demonstrated that the singlet ground state was achieved when the substituents are strong electron-withdrawing groups such as F or alkoxy group (OR) in which case type-1 TB interaction was adopted to increase the energy gap between the Ψ_A and Ψ_S. On the other hand, the small energy gap between Ψ_A and Ψ_S because of the high lying σ_{CH} leading to the increasing of energy level of Ψ_S, the triplet ground-state was obtained when the substituents are electro-donating groups (type-2).
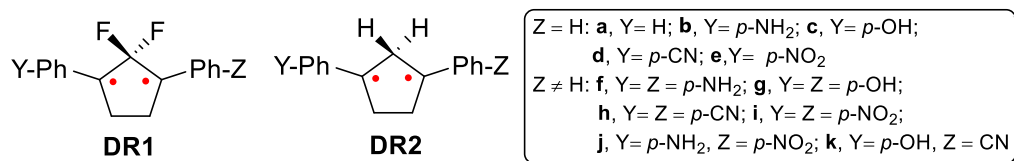
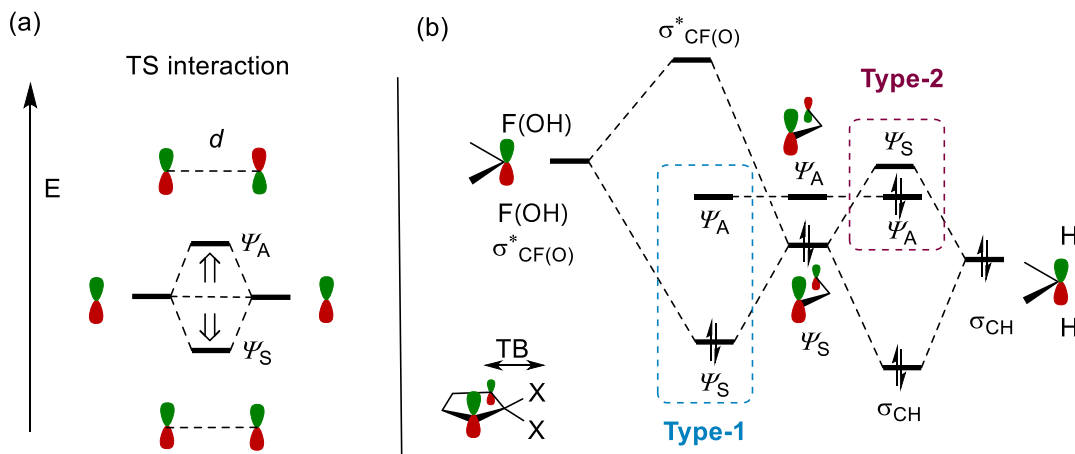**Figure 1.2.** The structures of **DR1** and **DR2**.

Figure 1.3. (a) Through-space (TS) interaction between the two p orbitals. (b) Through-bond (TB) interactions in diradicals: Type-1 and Type-2 interactions.

In addition, the confirmation of the ground state of diradicals was also implemented by the electron spin resonance (ESR) spectroscopy. Because the Zeeman effect does not be applied for singlet diradicals with zero value for the magnetic quantum number (m_s), the triplet state diradicals are only ESR-active species. Thus, the ESR is a powerful probe of the electronic nature of diradicals triplet state[21] and the triplet diradicals ESR signals determine the two zero-field splitting (zfs) parameters D and E. In 1975, the ESR spectrum of cyclopentane-1,3-diyl **DR3** (Figure 1.4) with $D/hc = -0.084$ cm^{-1} and $E/hc = \pm0.0020$ cm^{-1} was reported by Buchwalter and Close which is also the first directly observed localized diradical.[22] Since then, numerous studies about the ESR spectroscopic detection directly were reported. For instance, Adam *et al.* discovered that there is a relationship between D parameter and the spin densities (ρ) at the radical sites and inter-radical distance (d) by

theoretical analysis of the magnetic dipole interaction and the *D* parameter depends on spin density factor ρ allowing to assess electronic substituent effects quantitatively by the measurement of ESR signals for localized 1,3-cyclopentanediyl triplet diradicals (**DR4-6**) where the distance factor *d* is constant.[23] Later, they found the order of spin delocalization of the substituents and stabilization of the radical center (vinyl > phenyl > carbonyl >> alkyl) for cyclopentane-1,3-diyl triplet diradicals based on *D* parameters determined by ESR spectroscopy.[24] Very recently, unlike the triplet ground state for parent diradical, **DR-2Ph**,[25] the singlet ground state for **DR$_{endo}$-6CPP** featuring puckered structure arising from the curved paraphenylene moiety was examined by ESR spectroscopy.[26]
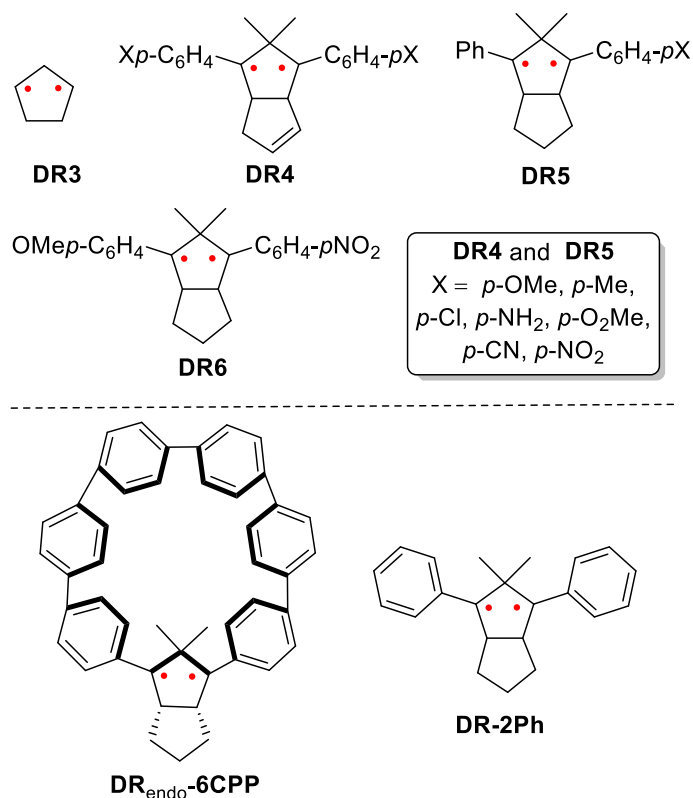

Figure 1.4. The structures of **DR3-6**, **DR-2Ph** and **DR$_{endo}$-6CPP**.

Chemical bond determining the three-dimensional molecular structure and electronic structure is so essential to a true appreciation of chemistry. As mentioned above, the localized diradicals are key intermediates in the bond-forming and bond-breaking processes.

Interestingly, localized singlet diradicals featuring π-single bond where π-bond without a σ-bond framework (Figure 1.5 a). Different from the typically stronger σ-bond with more effective in linear overlap of orbitals and π-bond with the sideways overlap of orbitals, π-single bond tends to isomerize into the singly σ-bond benefitting from the dramatically smaller HOMO–LUMO energy gap.[27–29] Continuous efforts have contributed to the emergence of a number of isolable π-single bonding molecules fusing heteronuclear bridging units. For example, an indefinitely stable singlet diradical fusion of heteroatom B has been achieved at room temperature by Bertrand *et al.* and the B–B distance is 2.57 Å which is about 1.38 times than that for the reported longest B–B bond (1.86 Å).[30,31] In 2020, a closed-shell compound with far longer Si–Si π single bond (2.853 Å) has been reported by Kyushin *et al.*.[32] Furthermore, studies on π-single bond consisting of bridgehead Si–Ge[33,34] and Ge–Ge[35] have also been disclosed abundantly during last decades (Figure 1.5b).
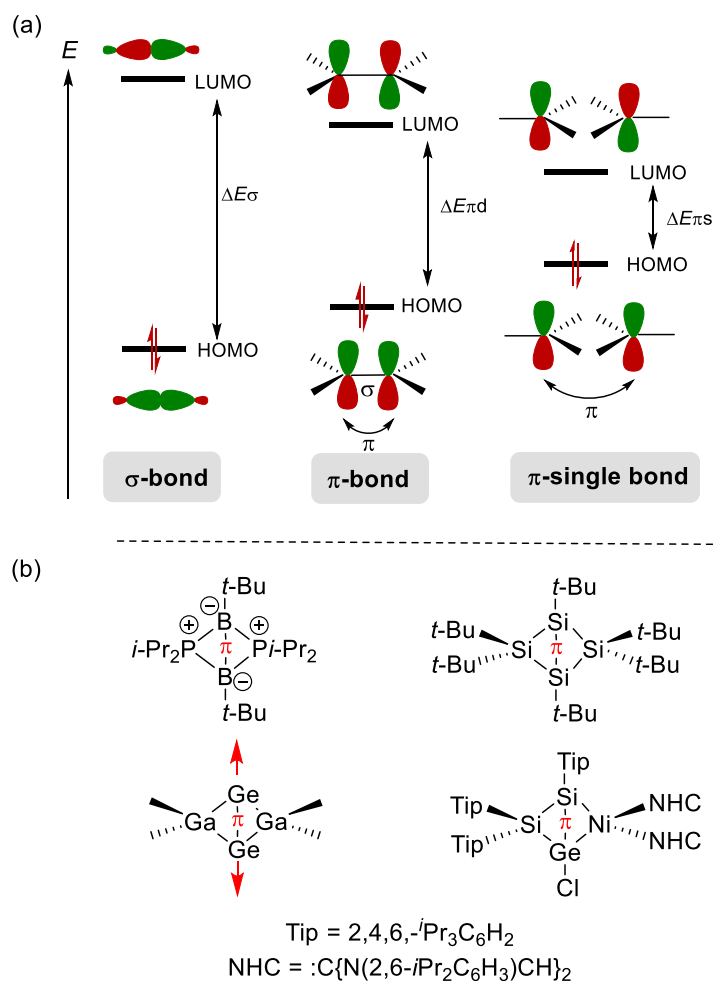
Figure 1.5. (a) Concepts of a σ-bond, π-bond and π-single bond. (b) Selected examples of structures of compounds containing heteronuclear with π-single bond.

Besides the characteristic π-single bond character, the zwitterionic feature also plays an important role in the reactivity of localized singlet diradicals (Figure 1.6a). A typical example is localized singlet diradical **DR7** (Figure 1.6b)[36–38] and the stabilization of **DR7** induced by novel nitrogen-atom effect affords the observation of thermal equilibrium between diradical and corresponding ring closed compound by time-resolved ultraviolet-visible (UV/Vis) and infrared (IR) spectroscopy. The smaller equilibrium constant K attributed to the increase of the energy barrier for the ring-closing reaction in polar solvent the demonstrated the zwitterionic characteristic of **DR7**.
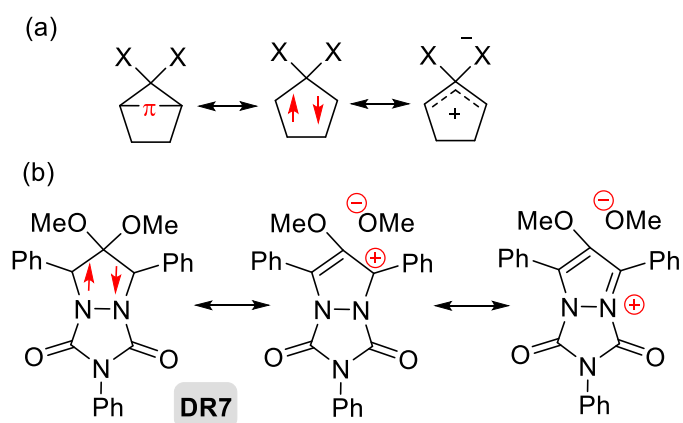
Figure 1.6. (a) Resonance structures of singlet diradcials. (b) Resonance structures of **DR7**.

1.2   The study of carbon-centered localized singlet diradicals

Unlike the triplet diradicals which have nanosecond time scale lifetime at room temperature,[39] the localized singlet diradicals recognized as putative (undetectable) intermediates because of the barrier-less processes for radical-radical coupling reaction leading to lifetime of less than 1ps.[40] Thus, there is much less knowledge about the localized singlet diradicals which encourages chemists to devoted to designing or isolating a persistent localized singlet diradical. Especially, there is growing interest in the generation and properties of carbon-centered localized singlet diradicals generated via fragmentation reaction with concomitant elimination of small molecules such as N_2 (Scheme 1.1) and some attractive strategies have been reported to construct them over the past few decades.
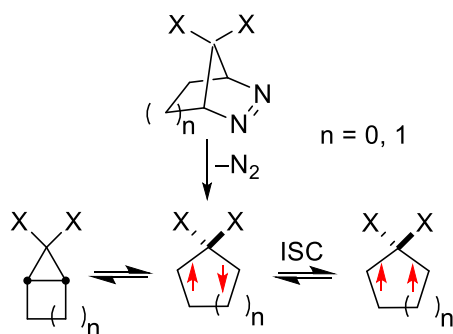
Scheme 1.1. Generation of cyclopentane-1,3-diyls and cyclobutane-

1,3-diyls.

As we have mentioned previously, different from triplet ground state hydrocarbon diradicals **DR2**, **DR1** were always singlet ground state theoretically regardless of the π-electron-donating and π-electron-withdrawing *para* substituents.[13] Similar result was also reported for the simplest 2,2-difluorocyclopentane diradical **DR8** (Figure 1.7). Although **DR3** has been confirmed the triplet ground state,[22] **DR8** was predicted to be singlet ground state with 11.2 kcal mol^{-1} lower than the triple one.[17] Experimentally, localized singlet diradical **DR9** was detected by the transient spectroscopy with a strong absorption around 530 nm and the lifetime value was 80 ns in *n*-pentane at room temperature.[41] Moreover, the log (A/s^{-1}) = 12.8 value which is much larger than that for triplet diradicals[42] was determined in cyclohexane for **DR9** suggesting the spin-allowed reaction. The singlet ground state was further proved by the ESR silent. In 2021, our laboratory observed the planar structure of **DR9** using steady-state infrared spectroscopy in an Ar matrix at 4 K and the IR and UV/Vis spectra disclosed the formation of cation **CT9**.[43]
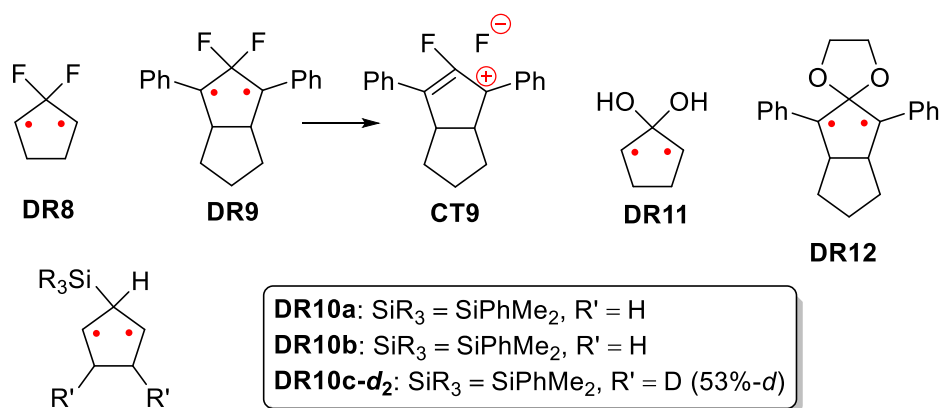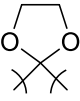

Figure 1.7. The structures of **DR8-12** and **CT9**.

Table 1.1. Substituents (X) effects on the ground state cyclopentane-1,3-diyls **DR**, at UB3LYP/6-31 G (d) level of theory.[17]

DR (X, X)	ΔE_{ST} / kcal mol^{-1}
DR3 (H, H)	+1.3
DR8 (F, F)	−11.2
DR13 (SiH$_3$, SiH$_3$)	−5.2
DR11 (OH, OH)	−6.7
DR14	−12.2

Apart from the geminal fluorine atom substituent preferring the singlet ground state, diradicals with silyl groups at C2 position also favor the singlet ground state with an obviously negative ΔE_{ST} although silyl groups belong to electron-donating substituents.[17,20,44] The substituent effect for silyl groups was attributed to the type-2 TB interaction of Ψ_S with high-lying occupied σ_{CSi} in which case destabilizes Ψ_S to energetically Ψ_A below Ψ_S (Figure 1.8). The detailed thermal and photochemical study has elucidated the singlet ground state for **DR10** (Figure 1.7).[45] Additionally, comparing with intramolecular cyclization, the silyl migration reaction was found to be significantly faster for **DR10**. It is noteworthy that the migration reaction in singlet **DR10** was also revealed by the deuterium labeling experiments.
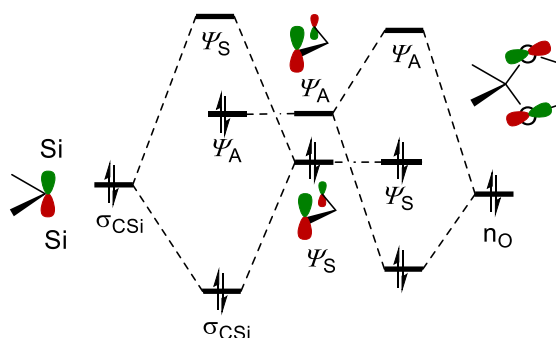
Figure 1.8. Orbital interactions for silyl and ethylene ketal substituted diradicals.

In 2004, Abe *et al.* reported the spiroconjugation effects on ΔE_{ST} and noted much negative ΔE_{ST} calculated value for the ethylene ketal substituted diradicals in comparison to the case of silyl or fluorine diradicals.[17,46] As clearly shown in Figure 1.8, orbital interaction gives us reasonable explanation that destabilization of Ψ_A induced by spiroconjugation of Ψ_A with lone pair orbital (n_O) of oxygen is the responsible for an increase of the energy gap between Ψ_A and Ψ_S. Interestingly, ΔE_{ST} was strongly affected by the O–C2–O–H dihedral angle for **DR11** (Figure 1.8). Experimentally, singlet diradical **DR12** was generated by photolysis of corresponding precursor azoalkane and the wavelength of first absorption band at around 514 nm measured in a methylcyclohexane (MCH)/2-methyltetrahydrofuran (MTHF) glass at 77 K.[46] To this end, as stated above, deriving from the zwitterionic resonance structure of singlet diradicals (Figure 1.6), the fusion of heteroatom such as nitrogen and silicon atoms is also useful strategy for achieving the localized singlet diradicals.[17,19]

1.3 The study of localized singlet 2,2-alkoxy-1,3-diyl diradicals

Alkoxy OR group as one of the most common electronegative substituents, understanding the role of OR in localized diradicals is therefore always a fundamental issue. Numerous studies including theoretical and experimental works have identified that consistent with fluorine atom F, OR substituents at C2 position result to localized singlet 2,2-alkoxy-1,3-diyl diradicals.[14]

The parent 2,2-dimethoxycyclopentane-1,3-diyl singlet diradicals **DR15** was generated by laser flash photolysis of azo **AZ15** in benzene at 293 K and strong absorption at $\lambda_{max} \approx 600$ nm assigned to **DR15** were detected in 2002.[47] The singlet ground state was also proved by the ESR silent at 77 K. In accordance with the F case, a large log $(A/s^{-1}) = 11.2$ value for **DR15** demonstrated the spin-allowed ring closing reaction.[47] Subsequently, experiments of stereoselectivity for the photodenitrogenation **AZ15** revealed the generation of two conformations

of photoproduct conformations inv-**CP15** and ret-**CP15** and the thermal isomerization between inv-**CP15** and ret-**CP15** was detected by NMR spectroscopy at 188 K under dark condition. Two distinct diradicals pucker puc-**DR15** and planar pl-**D15** involved in the photoreaction were indicated in the selection formation of ret-**CP15**. The detailed mechanism of the thermal and photochemical reaction for **AZ15** was analyzed reasonably (Figure 1.9a).[48,49] Actually, puckered structure localized singlet diradical **DR16** has been reported by our laboratory.[50] Different from typical absorption at around 580 nm for planar diradicals, the absorption band assigned to puc-**DR16** appears at around 450 nm at 98 K in MTHF (Figure 1.9b).
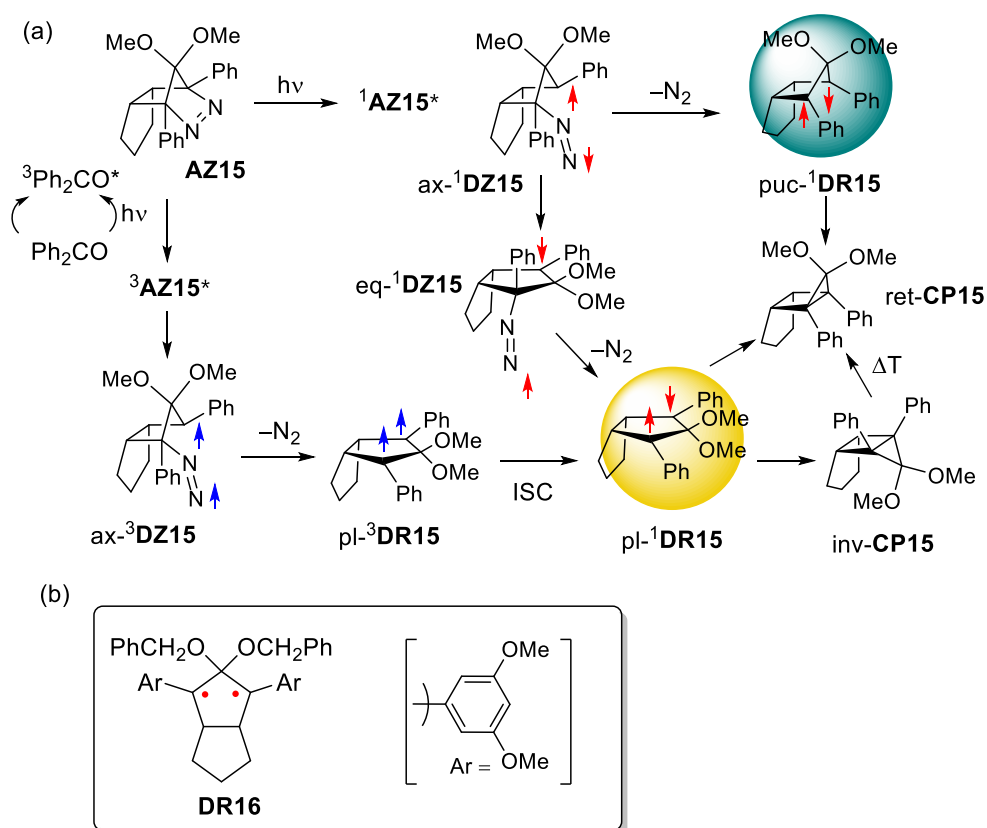

Figure 1.9. (a) Mechanism of spin-state dependent change in stereoselectivity in **AZ15** denitrogenation. (b) The structure of **DR16**.
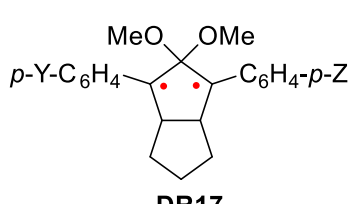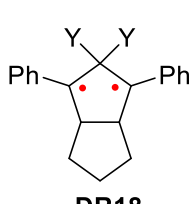
The high reactivity of localized singlet diradicals has provided challenges to investigate deeply of its chemical characteristics especially π single bond character. To observe singlet diradicals directly, strategies

for the construction of longer lifetime localized singlet diradicals with π single bond are indispensable. Examples of these strategies include electronic substituent effect, steric effect and stretch effect.

The electronic substituent effect for 2,2-dimethoxycyclopentane-1,3-diyl diradicals has been elucidated by Abe's work (Table 1.2).[47] Even though both electron-donating and withdrawing groups allowing for the longer lifetime of diradicals comparison of the parent diradical **DR15**, the electron-donating groups at the para position of phenyl rings exhibit more pronounced effect for symmetrical system due to the hyperconjugation, while the order of lifetime manifested for unsymmetrically substituted diradicals was attributed to the zwitterionic character of diradicals (Table 1.2).

Concerning the steric effect, study of the impact of alkoxy group on the lifetime of singlet diradicals showed the result that the lifetime increases with the increasing of carbon chain length of alkoxy groups which could be explained by the steric interaction between the alkoxy group and phenyl ring (Table 1.2).[51] However, the steric effect was quite small when the chain length over C3 of alkoxy group where moiety over C3 were far away from the nonbonded interaction according to the computational results (Table 1.2). Bulky substituent effect at *meta*-position of the phenyl ring in singlet 2,2-diethoxy-1,3-diarylcyclopentane-1,3-diyls where the lifetime was 45 times longer than that of parent the diradical (**DR19b**) when the substituent is bulky group triisopropylphenyl (**DR19a**, Figure 1.10a). [52]

Table 1.2. Substituents effects on the lifetime of cyclopentane-1,3-diyls **DR**.[47,51]

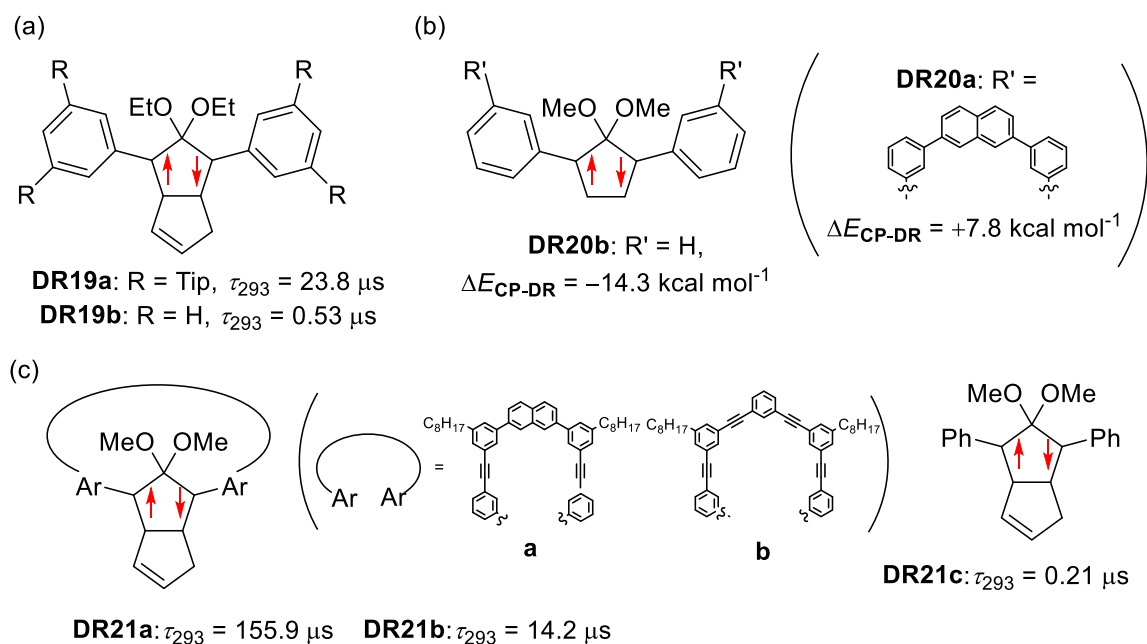| Structure	DR	τ_{293} / ns (benzene)
	DR15	320 ± 15
	a (Y, Z = OMe)	1050 ± 80
	b (Y, Z = Me)	460 ± 30
	c (Y, Z = Cl)	490 ± 30
	d (Y, Z = CN)	625 ± 25
	e (Y = OMe, Z = H)	600 ± 35
	f (Y = CN, Z = H)	470 ± 30
	g (Y = OMe, Z = CN)	740 ± 60
	a (Y = OC_2H_5)	880
	b (Y = OC_3H_7)	1899
	c (Y = OC_6H_{13})	2292
	d (Y = $OC_{10}H_{21}$)	2146

Figure 1.10. The structures of **DR19-21**.

Stretch effect is so called macrocycle effect caused by macrocycle ring which are desirable scaffold for adjusting the lifetime of diradicals.[53] Different from the kinetic stabilization and thermodynamic stabilization that design persistent diradicals by preventing intermolecular reaction and electron delocalization respectively, the stretch effect was found to thermodynamically destabilize corresponding the σ-bonded compounds of 1,3-diradicals and kinetically stabilize the diradicals. With the 2,7-naphlene unit doping into the macrocyclic system, the diradical **DR20a** was calculated to be considerably more stable than ring-closed compound, $\Delta E_{\text{CP-DR}}$ = +7.8 kcal mol^{-1} [53] whereas for the parent diradical **DR20b** without macrocyclic ring $\Delta E_{\text{CP-DR}}$ = −14.3 kcal mol^{-1} [17] (Figure 1.10b). Recently, our group reported the more examples of localized singlet diradicals stabilized kinetically by macrocyclic skeleton.[54–56] The lifetimes of diradicals **DR21a** (156 μs) and **DR21b** (14 μs) are approximately 800 and 70 times than the parent diradical **DR21c** (0.2 μs) without macrocycle structure at 293 K in benzene, respectively (Figure 1.10c).[54,55]

1.4 The study of this thesis

As aforementioned, the zwitterionic character about the localized singlet diradicals could lead to the smaller equilibrium constant K in polar solvents which corresponds to the ring-closing reaction of diradicals.[37,38] Therefore, the lifetime of singlet diradicals determined by the ring-closing reaction was expected to be strongly affected by the solvent polarity. In fact, relative study has been carried out for localized singlet 2,2-alkoxy-1,3-diyl diradicals by our group and the results has shed light on the relationship between lifetime and solvent polarity. For example, there is an almost linear relationship between lifetime of **DR19b** and solvent polarity.[57] However, the lifetime of diradicals is not only dependent on the solvent polarity.[55,58] This thesis will focus on the dynamic solvent effects on the lifetimes of localized single diradicals. In particular, in high viscous solvents, the traditional transition state theory (TST) cannot be applied to explain the transformation of molecule in

contrast the solvent fluctuation plays an important role in determining the rate constant of chemical reaction.[59,60] The investigation was investigated in 18 different solvents and solvent mixtures with very broadly range polarity (from −0.11 to 1 kcal mol^{-1}) and viscosity (from 0.24 to 125.4 mPa s) variation. Experimental evidence is displayed for the crucial roles of polarity and viscosity in isomerization of diradicals with π-single bonding character. Remarkably, it was discovered that in low-viscosity solvents (η < 1 mPa s), isomerization process described by lifetime parameter of diradicals is more dependent of solvent polarity. Conversely, viscosity governs isomerization of diradicals under high viscous solvents. Moreover, more pronounced viscosity effect for the singlet diradical with long carbon chain at remote position of the reaction sites suggested the cyclopentane moiety motion during the chemical isomerization.

Reference

(1) Salem, L.; Rowland, C. The Electronic Properties of Diradicals. *Angew. Chem., Int. Ed.* **1972**, 11, 92–111.

(2) Wang, C.; Hao, H.; Tajima, K. Essential Role of Triplet Diradical Character for Large Magnetoresistance in Quinoidal Organic Semiconductor with High Electron Mobility. *Adv. Sci.* **2022**, *9*, 2201045.

(3) Femoni, C.; Iapalucci, M. C.; Longoni, G.; Tiozzo, C.; Wolowska, J.; Zacchini, S.; Zazzaroni, E. New Hybrid Semiconductor Materials Based on Viologen Salts of Bimetallic Fe–Pt and Fe–Au Carbonyl Clusters: First Structural Characterization of the Diradical π-Dimer of the Diethylviologen Monocation and EPR Evidence of Its Triplet State. *Chem. - A Eur. J.* **2007**, *13*, 6544–6554.

(4) Chen, Z.; Li, W.; Sabuj, M. A.; Li, Y.; Zhu, W.; Zeng, M.; Sarap, C. S.; Huda, M. M.; Qiao, X.; Peng, X.; Ma, D.; Ma, Y.; Rai, N.; Huang, F. Evolution of the Electronic Structure in Open-Shell Donor-Acceptor Organic Semiconductors. *Nat. Commun.* **2021**, *12*, 5889.

(5) Wonink, M. B. S.; Corbet, B. P.; Kulago, A. A.; Boursalian, G. B.; de Bruin, B.; Otten, E.; Browne, W. R.; Feringa, B. L. Three-State Switching of an Anthracene Extended Bis-Thiaxanthylidene with a

Highly Stable Diradical State. *J. Am. Chem. Soc.* **2021**, *143*, 18020–18028.

(6) Muhammad, S.; Nakano, M.; Al-Sehemi, A. G.; Kitagawa, Y.; Irfan, A.; Chaudhry, A. R.; Kishi, R.; Ito, S.; Yoneda, K.; Fukuda, K. Role of a Singlet Diradical Character in Carbon Nanomaterials: A Novel Hot Spot for Efficient Nonlinear Optical Materials. *Nanoscale,* **2016**, *8*, 17998–18020.

(7) Enholm, E.; Joshi, A.; Wright, D. L. Photocurable Hard and Porous Biomaterials from ROMP Precursors Cross-Linked with Diyl Radicals. *Bioorg. Med. Chem. Lett.* **2005**, *15*, 5262–5265.

(8) Saha, B.; Ehara, M.; Nakatsuji, H. Investigation of the Electronic Spectra and Excited-State Geometries of Poly (*Para*-Phenylene Vinylene) (PPV) and Poly (*Para*-Phenylene) (PP) by the Symmetry-Adapted Cluster Configuration Interaction (SAC-CI) Method. *J. Phys. Chem. A* **2007**, *111*, 5473–5481.

(9) Borden, W. T.; Davidson, E. R. Effects of Electron Repulsion in Conjugated Hydrocarbon Diradicals. *J. Am. Chem. Soc.* **1977**, *99*, 4587–4594.

(10) Ess, D. H.; Johnson, E. R.; Hu, X.; Yang, W. Singlet−Triplet Energy Gaps for Diradicals from Fractional-Spin Density-Functional Theory. *J. Phys. Chem. A* **2011**, *115*, 76–83.

(11) Chambers, T. S.; Kistiakowsky, G. B. Kinetics of the Thermal Isomerization of Cyclopropane. *J. Am. Chem. Soc.* **1934**, *56*, 399–405.

(12) Hund, F. Z. *Phys.* **1925**, *33*, 345.

(13) Zhang, D. Y.; Hrovat, D. A.; Abe, M.; Borden, W. T. DFT Calculations on the Effects of *Para* Substituents on the Energy Differences between Singlet and Triplet States of 2,2-Difluoro-1,3-Diphenylcyclopentane-1,3-Diyls. *J. Am. Chem. Soc.* **2003**, *125*, 12823–12828.

(14) Abe, M. Diradicals. *Chem. Rev.* **2013**, *113*. 7011–7088.

(15) Getty, S. J.; Hrovat, D. A.; Borden, W. T. *Ab* Initio Calculations on the Stereomutation of 1,1-Difluorocyclopropane. Prediction of a Substantial Preference for Coupled Disrotation of the Methylene

Groups. *J. Am. Chem. Soc.* **1994**, *116*, 1521–1527.

(16) Xu, J. D.; Hrovat, D. A.; Borden, W. T. *Ab* Initio Calculations of the Potential Surfaces for the Lowest Singlet and Triplet States of 2,2-Difluorocyclopentane-1,3-Diyl. The Singlet Diradical Lies Below the Triplet. *J. Am. Chem. Soc.* **1994**, *116*, 5425–5427.

(17) Abe, M.; Ye, J.; Mishima, M. The Chemistry of Localized Singlet 1,3-Diradicals (Biradicals): From Putative Intermediates to Persistent Species and Unusual Molecules with a π-Single Bonded Character. *Chem. Soc. Rev.,* **2012**, *41*, 3808–3820.

(18) Hoffmann, R. Trimethylene and the Addition of Methylene to Ethylene. *J. Am. Chem. Soc.* **1968**, *90*, 1475–1485.

(19) Nakamura, T.; Gagliardi, L.; Abe, M. Computational Study of the Cooperative Effects of Nitrogen and Silicon Atoms on the Singlet-Triplet Energy Spacing in 1,3-Diradicals and the Reactivity of Their Singlet States. *J. Phys. Org. Chem.* **2010**, *23*, 300–307.

(20) Abe, M.; Ishihara, C.; Nojima, M. DFT Prediction of Ground-State Spin Multiplicity of Cyclobutane-1,3-Diyls: Notable Effects of Two Sets of Through-Bond Interactions. *J. Org. Chem.* **2003**, *68*, 1618–1621.

(21) Wasserman, E.; Hutton, R. S. Electron Paramagnetic Resonance of Triplet States: Cyclic 4π-Electron Systems, CH_2, and Environmental Effects. *Acc. Chem. Res.* **1977**, 27–32.

(22) Buchwalter, S. L.; Closs, G. L. An Electron Spin Resonance Study of Matrix Isolated 1,3-Cyclopentadiyl, a Localized 1,3-Carbon Biradical. *J. Am. Chem. Soc.* **1975**, *97*, 3857–3858.

(23) Adam, W.; Kita, F.; Harrer, H. M.; Nau, W. M.; Zipf, R. The *D* Parameter (EPR Zero-Field Splitting) of Localized 1,3-Cyclopentanediyl Triplet Diradicals as a Measure of Electronic Substituent Effects on the Spin Densities in *Para*-Substituted Benzyl-Type Radicals. *J. Org. Chem.* **1996**, *61*, 7056–7065.

(24) Adam, W.; Emmert, O.; Heidenfelder, T. The EPR-Spectral *D* Parameter of Photochemically Generated Cyclopentane-1,3-Diyl Triplet Diradicals as a Quantitative Measure of Spin Delocalization in Vinyl-, Phenyl-, and Carbonyl-Substituted Radicals. *J. Org. Chem.*

1999, *64*, 3417–3421.

(25) Adam, W.; van Barneveld, C.; Emmert, O. The EPR *D* Parameter as a Measure of Spin Delocalization in Cyclopentane-1,3-Diyl Triplet Diradicals with Extended Conjugation π-Type Substituents. *J. Chem. Soc., Perkin Trans. 2,* **2000**, 637–641.

(26) Miyazawa, Y.; Wang, Z.; Matsumoto, M.; Hatano, S.; Antol, I.; Kayahara, E.; Yamago, S.; Abe, M. 1,3-Diradicals Embedded in Curved Paraphenylene Units: Singlet versus Triplet State and In-Plane Aromaticity. *J. Am. Chem. Soc.* **2021**, *143*, 7426–7439.

(27) Jemmis, E. D.; Pathak, B.; King, R. B.; Schaefer III, H. F. Bond Length and Bond Multiplicity: σ-Bond Prevents Short π-Bonds. *Chem. Commun.* **2006**, 20, 2164–2166.

(28) Nukazawa, T.; Iwamoto, T. π-Conjugated Species with an Unsupported Si–Si π-Bond Obtained from Direct π-Extension. *Chem. Commun.* **2021**, *57*, 9692–9695.

(29) Hinz, A.; Kuzora, R.; Rölke, A.; Schulz, A.; Villinger, A.; Wustrack, R. Synthesis of a Silylated Phosphorus Biradicaloid and Its Utilization in the Activation of Small Molecules. *Eur. J. Inorg. Chem.* **2016**, *2016*, 3611–3619.

(30) Scheschkewitz, D.; Amii, H.; Gornitzka, H.; Schoeller, W. W.; Bourissou, D.; Bertrand, G. Singlet Diradicals: From Transition States to Crystalline Compounds. *Science,* **2002**, *295*, 1880–1881.

(31) Pilz, M.; Allwohn, J.; Willershausen, P.; Massa, W.; Berndt, A. 2,3-Diboratabutadienes and 2-Borataallenes. *Angew. Chem. Int. Ed. Engl.* **1990**, *29*, 1030–1032.

(32) Yang, W.; Zhang, L.; Xiao, D.; Feng, R.; Wang, W.; Pan, S.; Zhao, Y.; Zhao, L.; Frenking, G.; Wang, X. A Diradical Based on Odd-Electron σ-Bonds. *Nat. Commun.* **2020**, *11*, 3441.

(33) Majhi, P. K.; Zimmer, M.; Morgenstern, B.; Scheschkewitz, D. Transition-Metal Complexes of Heavier Cyclopropenes: Non-Dewar–Chatt–Duncanson Coordination and Facile Si=Ge Functionalization. *J. Am. Chem. Soc.* **2021**, *143*, 8981–8986.

(34) Lee, V. Ya.; Ichinohe, M.; Sekiguchi, A.; Takagi, N.; Nagase, S. The First Three-Membered Unsaturated Rings Consisting of Different

Heavier Group 14 Elements: 1-Disilagermirene with a Si=Si Double Bond and Its Isomerization to a 2-Disilagermirene with a Si=Ge Double Bond. *J. Am. Chem. Soc.* **2000**, *122*, 9034–9035.

(35) Doddi, A.; Gemel, C.; Winter, M.; Fischer, R. A.; Goedecke, C.; Rzepa, H. S.; Frenking, G. Low-Valent Ge_2 and Ge_4 Species Trapped by N-Heterocyclic Gallylene. *Angew. Chem. Int. Ed.* **2013**, *52*, 450–454.

(36) Abe, M.; Kubo, E.; Nozaki, K.; Matsuo, T.; Hayashi, T. An Extremely Long-Lived Singlet 4,4-Dimethoxy-3,5-Diphenylpyrazolidine-3,5-Diyl Derivative: A Notable Nitrogen-Atom Effect on Intra- and Intermolecular Reactivity. *Angew. Chem.* **2006**, *118*, 7992–7995.

(37) Yoshidomi, S.; Mishima, M.; Seyama, S.; Abe, M.; Fujiwara, Y.; Ishibashi, T. Direct Detection of a Chemical Equilibrium between a Localized Singlet Diradical and Its σ-Bonded Species by Time-Resolved UV/Vis and IR Spectroscopy. *Angew. Chem. Int. Ed.* **2017**, *56*, 2984–2988.

(38) Yoshidomi, S.; Abe, M. 1,2-Diazacyclopentane-3,5-Diyl Diradicals: Electronic Structure and Reactivity. *J. Am. Chem. Soc.* **2019**, *141*, 3920–3933.

(39) Adam, W.; Grabowski, S.; Wilson, R. M. Localized Cyclic Triplet Diradicals. Lifetime Determination by Trapping with Oxygen. *Acc. Chem. Res.* **1990**, *23*, 165–172.

(40) Pedersen, S.; Herek, J. L.; Zewail, A. H. The Validity of the "Diradical" Hypothesis: Direct Femtosecond Studies of the Transition-State Structures. *Science* **1994**, *266*, 1359–1364.

(41) Adam, W.; Borden, W. T.; Burda, C.; Foster, H.; Heidenfelder, T.; Heubes, M.; Hrovat, D. A.; Kita, F.; Lewis, S. B.; Scheutzow, D.; Wirz, J. Transient Spectroscopy of a Derivative of 2,2-Difluoro-1,3-Diphenylcyclopentane-1,3-Diyl-A Persistent Localized Singlet 1,3-Diradical. *J. Am. Chem. Soc.* **1998**, *120*, 593–594.

(42) Adam, W.; Reinhard, G. Effect of 2,2-Dimethyl Substitution on the Lifetimes of Cyclic Hydrocarbon Triplet 1,3-Biradicals. *J. Am. Chem. Soc.* **1990**, *112*, 4570–4571.

(43) Sarkar, S. K.; Abe, M. Direct Detection of Singlet Cyclopentane-1,3-Diyl Diradicals by Infrared and Ultraviolet–Visible Spectroscopy at Cryogenic Temperature and Their Photoreactivity. *J. Org. Chem.* **2021**, *86*, 12046–12053.

(44) Abe, M.; Akisaka, R. Is π-Single Bonding (C–π–C) Possible? A Challenge in Organic Chemistry. *Chem. Lett.* **2017**, *46*, 1586–1592.

(45) Abe, M.; Kawanami, S.; Ishihara, C.; Nojima, M. 2-Silyl Group Effect on the Reactivity of Cyclopentane-1,3-Diyls. Intramolecular Ring-Closure versus Silyl Migration. *J. Org. Chem.* **2004**, *69*, 5622–5626.

(46) Abe, M.; Adam, W.; Nau, W. M. Photochemical Generation and Methanol Trapping of Localized 1,3 and 1,4 Singlet Diradicals Derived from a Spiroepoxy-Substituted Cyclopentane-1,3-Diyl. *J. Am. Chem. Soc.* **1998**, *120*, 11304–11310.

(47) Abe, M.; Adam, W.; Hara, M.; Hattori, M.; Majima, T.; Nojima, M.; Tachibana, K.; Tojo, S. On the Electronic Character of Localized Singlet 2,2-Dimethoxycyclopentane-1,3-Diyl Diradicals: Substituent Effects on the Lifetime. *J. Am. Chem. Soc.* **2002**, *124*, 6540–6541.

(48) Abe, M.; Tada, S.; Mizuno, T.; Yamasaki, K. Impact of Diradical Spin State (Singlet vs Triplet) and Structure (Puckered vs Planar) on the Photodenitrogenation Stereoselectivity of 2,3-Diazabicyclo[2.2.1]Heptanes. *J. Phys. Chem. B* **2016**, *120*, 7217–7226.

(49) Abe, M.; Hatano, S. Mechanistic Study of Stereoselectivity in Azoalkane Denitrogenations. *Pure Appl. Chem.* **2017**, *89*, 759–764.

(50) Ye, J.; Hatano, S.; Abe, M.; Kishi, R.; Murata, Y.; Nakano, M.; Adam, W. A Puckered Singlet Cyclopentane-1,3-Diyl: Detection of the Third Isomer in Homolysis. *Chem. -A Eur. J.* **2016**, *22*, 2299–2306.

(51) Nakagaki, T.; Sakai, T.; Mizuta, T.; Fujiwara, Y.; Abe, M. Kinetic Stabilization and Reactivity of π Single-Bonded Species: Effect of the Alkoxy Group on the Lifetime of Singlet 2,2-Dialkoxy-1,3-Diphenyloctahydropentalene-1,3-Diyls. *Chem. -A Eur. J.* **2013**, *19*, 10395–10404.

(52) Akisaka, R.; Abe, M. Bulky Substituent Effect on Reactivity of Localized Singlet Cyclopentane-1,3-diyls with π-Single Bonding (C-π-C) Character. *Chem. Asian J.* **2019**, *14*, 4223–4228.

(53) Abe, M.; Furunaga, H.; Ma, D.; Gagliardi, L.; Bodwell, G. J. Stretch Effects Induced by Molecular Strain on Weakening σ-Bonds: Molecular Design of Long-Lived Diradicals (Biradicals). *J. Org. Chem.* **2012**, *77*, 7612–7619.

(54) Wang, Z.; Yadav, P.; Abe, M. Long-Lived Localised Singlet Diradicaloids with Carbon–Carbon π-Single Bonding (C–π–C). *Chem. Commun.* **2021**, *57*, 11301–11309.

(55) Wang, Z.; Akisaka, R.; Yabumoto, S.; Nakagawa, T.; Hatano, S.; Abe, M. Impact of the Macrocyclic Structure and Dynamic Solvent Effect on the Reactivity of a Localised Singlet Diradicaloid with π-Single Bonding Character. *Chem. Sci.,* **2021**, *12*, 613–625.

(56) Harada, Y.; Wang, Z.; Kumashiro, S.; Hatano, S.; Abe, M. Extremely Long Lived Localized Singlet Diradicals in a Macrocyclic Structure: A Case Study on the Stretch Effect. *Chem. -A Eur. J.* **2018**, *24*, 14808–14815.

(57) Akisaka, R.; Ohga, Y.; Abe, M. Dynamic Solvent Effects in Radical–Radical Coupling Reactions: An Almost Bottleable Localised Singlet Diradical. *Phys. Chem. Chem. Phys.,* **2020**, *22*, 27949–27954.

(58) Abe, M.; Adam, W.; Heidenfelder, T.; Nau, W. M.; Zhang, X. Intramolecular and Intermolecular Reactivity of Localized Singlet Diradicals: The Exceedingly Long-Lived 2,2-Diethoxy-1,3-Diphenylcyclopentane-1,3-Diyl. *J. Am. Chem. Soc.* **2000**, *122*, 2019–2026.

(59) Kramers, H. A. Brownian Motion in a Field of Force and the Diffusion Model of Chemical Reactions. *Physica,* **1940**, *7*, 284–304.

(60) Sumi, H. Theory on Reaction Rates in Nonthermalized Steady States during Conformational Fluctuations in Viscous Solvents. *J. Phys. Chem.* **1991**, *95*, 3334–3350.

Chapter 2.
Dynamic Solvent Effect on the Lifetime of Singlet Diradicals with π-Single Bonding

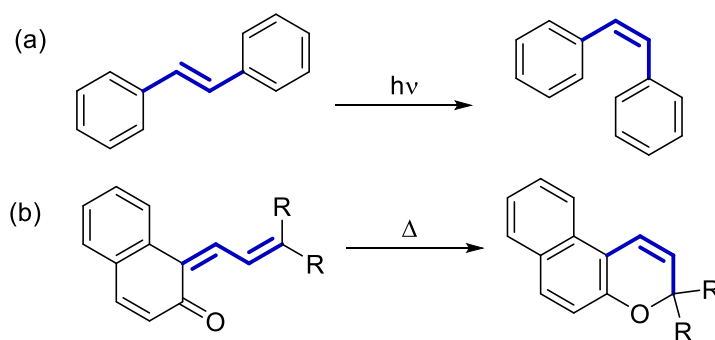## 2.1 Solvent effect on the isomerization reaction

Localized singlet diradicals featuring π-single bonding character, as key intermediates in the homolytic bond cleavage and formation reactions, have attracted significant attention in their structures, reactivity and kinetic stabilization. In 2000, our laboratory explored the intramolecular and intermolecular reactivity of localized singlet diradical S-**DR1** and found photoisomerization of localized singlet diradicals can be strongly influenced by solvents (Scheme 2.1).[1] Specifically, the lifetime of S-**DR1** determined by the rate constant of ring closing reaction decreased roughly with solvent polarity and the moderately linear relationship between the lifetimes and polarity values were observed. However, there are still some points deviating from the roughly linear correlation which suggested the lifetime value of diradical could not be explained by solvent polarity only.
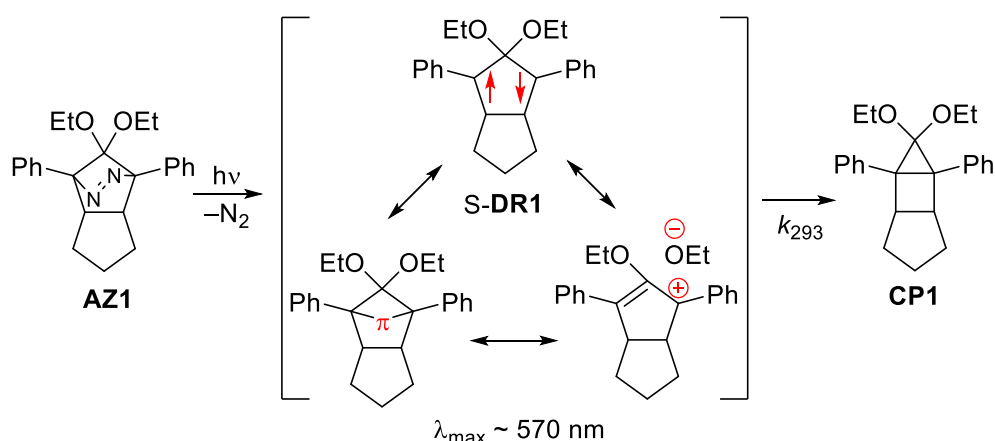
Scheme 2.1. Generation of the singlet diradical S-**DR1** in the photolysis of the azoalkane **AZ1** and the isomerization of S-**DR1** to the ring-closing compound **CP1**.

As we already known, the lifetime of diradical corresponds to the isomerization reaction from planar singlet diradical to the ring closing compound.[2–4] Date back to isomerization reaction, one of the most well-known reactions in chemistry, much effort was devoted to employing thermal and light-induced isomerization reactions in solvents and the results also suggest that solvents play a pivotal role in molecular transformations.[5–17] For example, the experimental studies of photoisomerization dynamics of stilbenes in solvents

demonstrate that the isomerization rate is sensitive to solvent polarity due to the polarizable character of transition state (Scheme 2.2a).[18] Furthermore, the rate of photoisomerization reaction was reported to be strongly affected by solvent viscosity where slower isomerization rate of stilbenes stems from an increasing solvent viscosity.[19–22] Especially, in highly viscous solvents, slow thermal fluctuations of solvents molecules lead to limited reaction rate allowing the observation of impressive dynamic solvent effect. Another typical example of dynamic solvent effects is the thermal cyclization of 1-prop-2-enylidenenaphthalen-2-one derivatives (Scheme 2.2b). Previous studies show that dynamic solvent effects for thermal ring closure are described by a two-dimensional model inclusion of medium and the chemical coordinate.[23] In 2016, the dynamic solvent effect on the thermal isomerization for this derivative (R = Ph) was observed firstly in ionic liquid and the reaction rates were retarded with increasing pressure causing high viscosity.[24] It is worth noting that dynamic solvent effects can be served as powerful tool to explore relative mobility of molecular moieties.[25,26] Asano and Ohga *et al.* revealed that instead of naphthalenone moiety, relative mobility of the ethenyl moiety governed the cyclization in the isomerization of 1-prop-2-enylidenenaphthalen-2-one derivatives.[26]

Scheme 2.2. Dynamic solvent effect on the (a) Isomerization of stilbene. (b) Isomerization of 1-prop-2-enylidenenaphthalen-2-one derivatives to 3*H*-naphtho[2,1-b]pyrans.

Dynamic solvent effects original from the friction between the molecules in solvents. Two-dimensional reaction coordinate model namely the reaction system and the solvents has been proposed for depicting the reaction.[5,27] The reaction is based on a two-step mechanism, Eq.1, where R, I and P are the

reactant, intermediate and product respectively, while k_f is fluctuation-limited constant.

$$R \underset{k_{-f}}{\overset{k_f}{\rightleftharpoons}} I \overset{k_1}{\longrightarrow} P \qquad (1)$$

One coordinate involved in the rate constants k_f and k_{-f} describes relatively slow thermal fluctuations on the energy surface of reactant. The second coordinate is composed of the rate constant k_1 controlled by atomic vibrational motions depicting energy barrier crossing. Before the second step representing chemical change to the product, solvent molecules are assumed to be rearranged by thermal fluctuation firstly to form a suitable configuration while the reactant keeps on its energy surface.[28,29] The whole reaction process in solvents is evaluated by the comparison of the observed rate constant k_{obs} with k_{TST} directly, Eq. 2.

$$1/k_{obs} = 1/k_{TST} + 1/k_f \qquad (2)$$

In low viscosity, considering the rapid solvent thermal fluctuations, the solvent can instantly follow the evolution of the reaction system in which case the reaction system was capable of obeying transition state theory (TST) and the $k_{obs} \approx k_{TST} = k_1$. In high viscous solvent, owing to the relatively slow solvent fluctuations comparing with the structural change of the reactant, which further causes the deactivation of the TST and the rate of reaction would be definitely influenced by the solvent viscosity, in other words, $k_{obs} \approx k_f$. Based on an Eq.3 and 4 in high viscous solvents (η and η_0 represent the viscosities at the pressures P and 0), so high pressure can be expected to be a promising method, aiming to effectively change in rate constant of the reaction. [16,30]

$$k_f \propto \eta^{-\beta}, 0 < \beta < 1 \qquad (3); \quad \eta = \eta_0 \exp(\alpha P) \qquad (4)$$

Dynamic solvent effects of localized singlet diradicals S-**DR2** featuring bulky aryl groups on the rate constant in isomerization was investigated under high pressure by our laboratory and an almost linear relationship between the solvent viscosity and lifetime was observed in various solvents (Scheme 2.3a).[31] Thus, the lifetime of S-**DR2** was predominantly governed by the solvent

viscosity under high-pressure conditions and it is noteworthy that the lifetime of S-**DR2** can be extremely extended to 2 s at room temperature in 2,4-dicyclohexyl-2-methyl pentane (DCMP) under high-pressure conditions. In 2021, regression analysis in dynamic solvent effect research was performed for diradicals S-**DR3a** and S-**DR3b** and comparison of the resulting regression analysis supported the fact that the solvent viscosity effect is more pronounced in the ring-closing of S-D**R3a** relative to S-**DR3b** lacking macrocycle ring (Scheme 2.3b).[32]
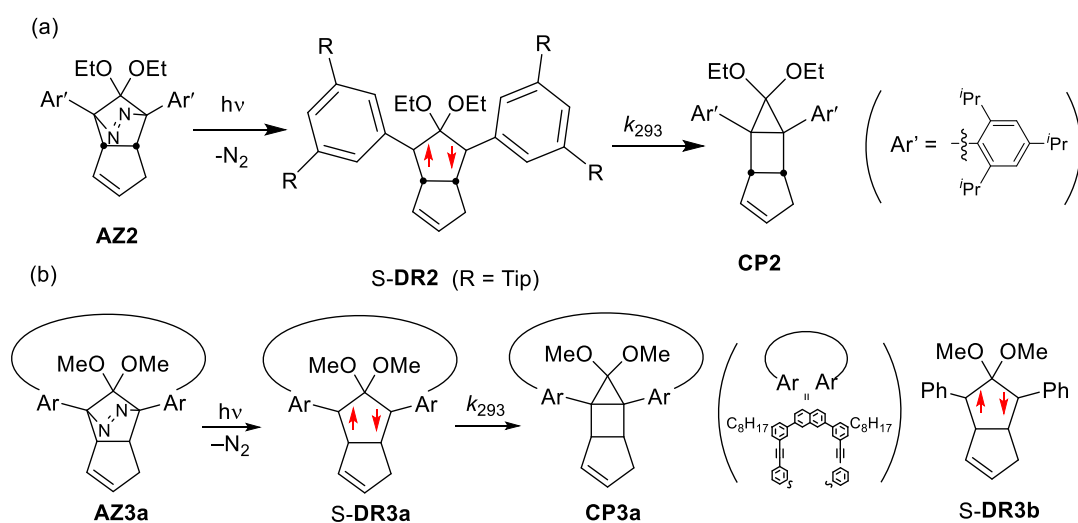
Scheme 2.3. (a) Generation of and isomerization of S-**DR2** featuring a bulky substituent. (b) Generation and isomerization of S-**DR3a** featuring a macrocyclic structure and structure of S-**DR3b**.

Encouraged by results from the dynamic solvent effects in isomerization of localized singlet diradicals with macrocycle and bulky substituents, herein, we continue our interest and explore the dynamic solvent effect of localized singlet diradicals S-**DR4a** and S-**DR4b** in 18 different solvents to evaluate long carbon chain on the dynamic solvent effect (Scheme 2.4). We have chosen binary mixture containing ionic liquid 1-Butyl-3-methylimidazolium hexafluorophosphate [BMIM][PF$_6$] and organic solvents glycerin triacetate (GTA) and dimethyl sulfoxide (DMSO) and a variety of organic solvents as liquid mediums, which permits a sufficiently broad change in the viscosity and polarity values. Meanwhile, during isomerization process from singlet diradicals with π-single bonding character to σ-single bonding species (from

planar S-**DR** to *trans* **CP**), at least two moieties change their relative positions in solvents.[3] Viscosity effect as a powerful tool provides the opportunity to elucidate relative mobilities of molecular moieties for the isomerization, therefore, S-**DR5** with long carbon chain at remote position from the reactive center was designed.


a: R = CH$_3$, **b**: R = (CH$_2$)$_9$CH$_3$

R = R = (CH$_2$)$_9$CH$_3$
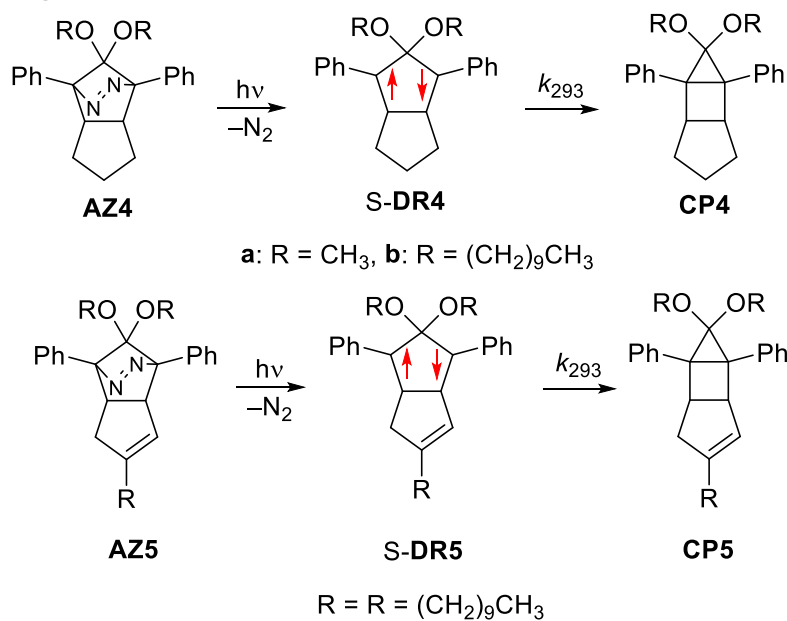
Scheme 2.4. Generation of and isomerization of S-**DR4** and S-**DR5**.

2.2 The synthesis and photoproduct analysis of azo precursor AZ5

The synthesis of azoalkanes **AZ4** has been reported in the previous literature.[3] Herein, following with similar the synthetic route of **AZ4**, a new azoalkane **AZ5** was prepared (Scheme 2.5). 1-Decanol and 1,1'-carbonyldiimidazole as the starting compounds synthesize didecyl carbonate **1** and then hydrazinolysis of **1** was performed to give compound **2**. Next, condensation of **2** with acetone were carried out and subsequently, oxidative cyclization leads to **4**. The [4+1] cycloaddition of **4** with diphenyltetrazine and following denitrogenation provided 4,4-dialkoxypyrazole (**5**). Next, the Diels–Alder cycloaddition was performed for **5** with 10 equiv of mixture decylcyclopenta-1,3-dienes **7** and **8** delivering azoalkane **AZ5** with only *trans* conformation.[33] The molecular structure of **AZ5** was identified by nuclear

magnetic resonance spectroscopy (^{1}H and ^{13}C NMR, Figures S2.5-2.6) including nuclear Overhauser effect measurements (NOE, Figure S2.7) and ESI mass spectrometry (MS, Figure S2.8). The cyclopentane moiety cannot be achieved by hydrogenation of **AZ5** under a H$_2$ atmosphere with Pd/C.
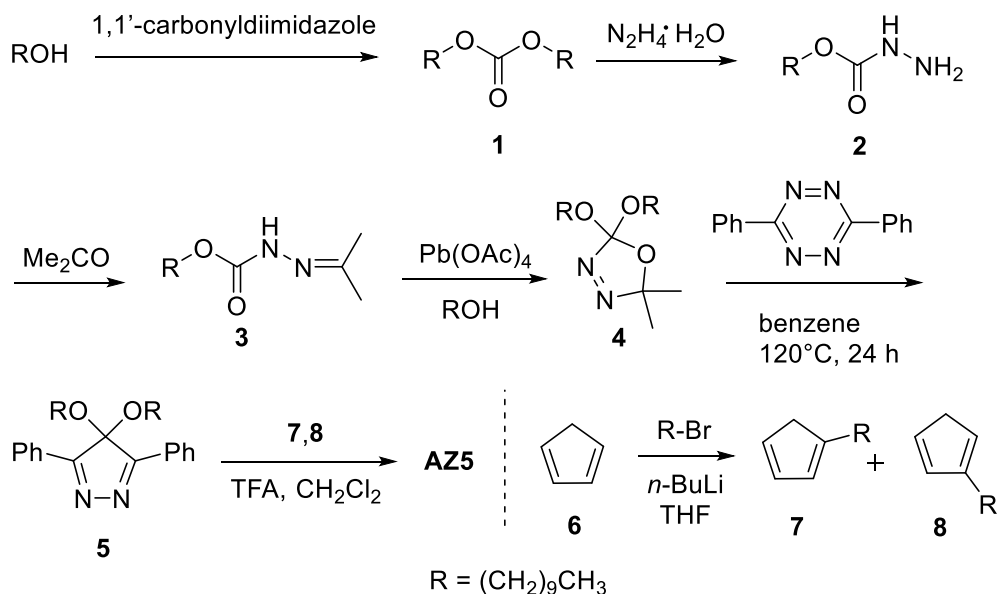
Scheme 2.5. Synthesis of **AZ5**.

In order to confirm the structure of photoproduct of **AZ5**, photodenitrogenation of **AZ5** (11.1 mM) was carried out by LED lamp (λ_{exc} = 365 nm) in C$_6$D$_6$ in a sealed NMR tube under a N$_2$ atmosphere at 298 K. As clearly shown in Figure 2.1, ring-closed product **CP5** was generated quantitatively and the *trans* configuration of **CP5** was proved by the directly analysis of nuclear Overhauser effect measurements. (NOE, Figure 2.1 inset) where the correlation between the bridgehead protons and alkoxy group was exhibited.
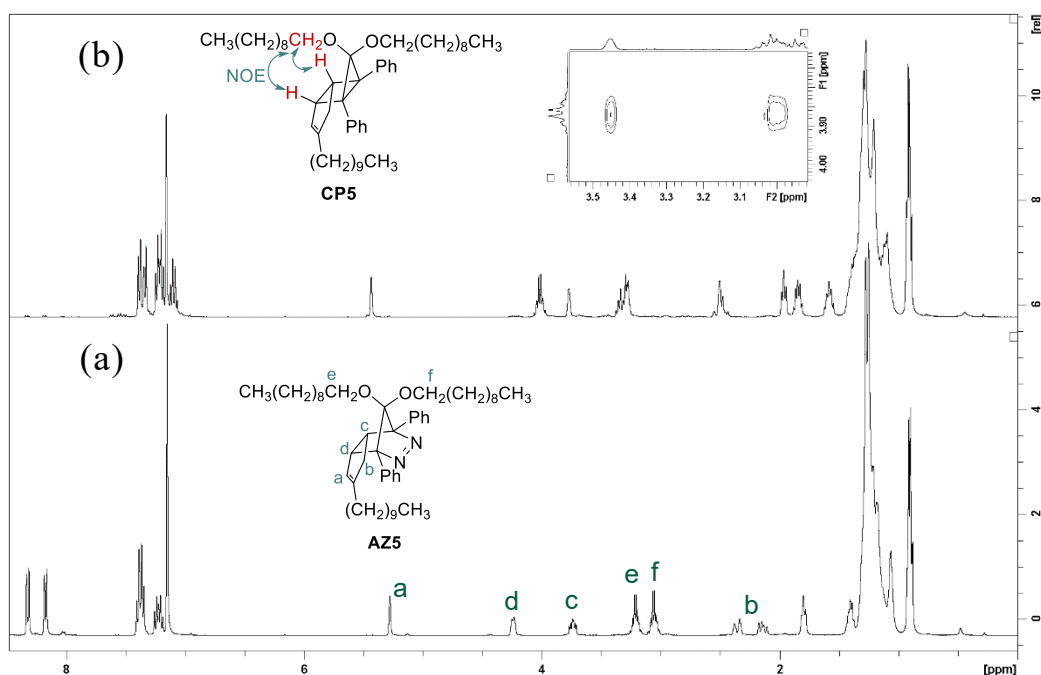
Figure 2.1. In suit ^{1}H NMR (400 MHz) analysis of the photodenitrogenation of **AZ5** (11.1 mM in C_6D_6). (a) **AZ5** before irradiation; (b) *trans*-**CP5** after irradiation. Inset: NOE measurement of **CP5** in CDCl$_3$.

2.3 The dynamic solvent effect on the lifetime of singlet diradicals

It is known that the localized singlet diradicals having π-single bonding character were determined by transient absorption spectroscopy when the alkoxy group was located at C2 position. The typical strong absorption at around 570 nm which was assigned to the HOMO (ψ_S)−LUMO (ψ_A) electronic excitation of the π-single bonding moiety of localized singlet diradicals could be detected.[3,34,35] Thereby, to explore the dynamic solvent effect, the transient absorption spectra and decay traces were measured under nitrogen condition firstly by the laser flash photolysis (LFP) with 355 nm laser (~5 mJ/pluse, 5 ns pulse width) at 293 K in seven low viscous solvents with different polarities (Table 2.1, entries 1−7; Figure 2.2). The lifetime (τ_{293}) values of S-**DR4a** and S-**DR4b** were obtained by first-order exponential fitting of the decay signals

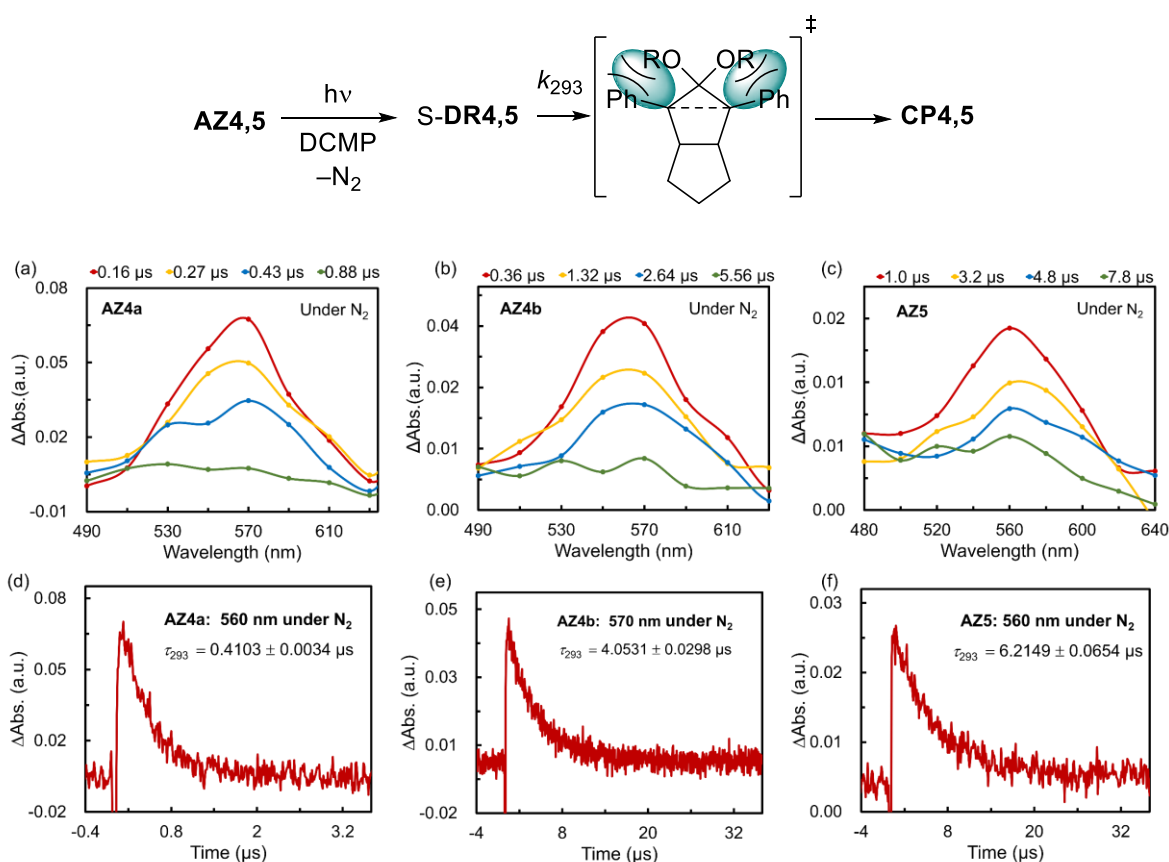at 560 nm and 570 nm, respectively.

Figure 2.2. Sub-microsecond transient absorption spectra during the laser flash photolysis of (a) **AZ4a**, (b) **AZ4b**, and (c) **AZ5** at 293 K in 2,4-dicyclohexyl-2-methyl pentane (DCMP, η = 38.7 mPa s) (entry 9, Table 2.1). (d) Time profile of S-**DR4a** at 560 nm, (e) Time profile of S-**DR4b** at 570 nm, (f) Time profile of S-**DR5** at 560 nm under a N_2 atmosphere.

As shown in Table 2.1, owing to the steric interaction between the Ph and OR groups in the transition state for isomerization process from the diradicals to ring-closing compounds, the lifetimes of S-**DR4b** were approximate 10 times longer than those of S-**DR4a** which is consistent with the previously reported results.[3] Moreover, lifetimes for both two diradicals tended to increase as the polarity increased and the polarity dependence is clearly noticed in the lifetimes of diradicals versus polarity plots in Figure 2.3 (a), although comparing with S-**DR4b** (R^2 = 0.73), the

better correlation suggested by the more higher coefficient value ($R^2 = 0.89$) was observed for S-**DR4a**. However, the very low coefficient values (0.36 and 0.27) in Figure 2.3b demonstrated the nonlinear correlation between lifetime values and viscosity for S-**DR4a** and S-**DR4b** in low viscous solvents.
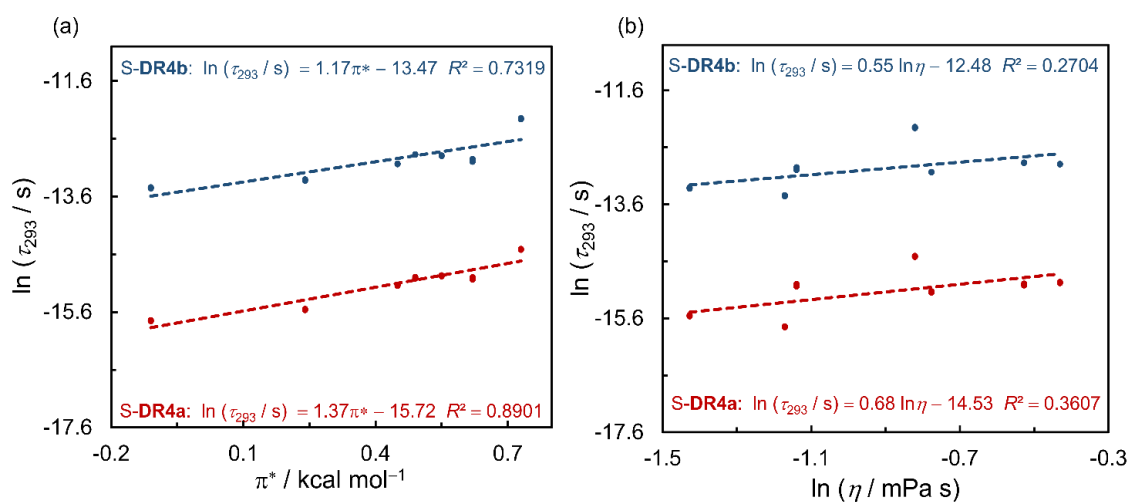

Figure 2.3. Correlations between the lifetimes (τ_{293}) of S-**DR4a** and S-**DR4b** with (a) polarity (π^*) and (b) viscosity (η) at 293 K in low-η ($\eta <$ 1 mPa s) organic solvents (entries 1−7).

Table 2.1. Lifetimes (τ_{293}) of the singlet diradicals S-**DR4a**, S-**DR4b**, and S-**DR5** at 293 K in different solvents.

Entry	Solvent	π^*/ kcal mol^{-1}	η / mPa s	S-**DR4a** $\tau_{293}/\mu s^a$	S-**DR4b** $\tau_{293}/\mu s^a$	S-**DR5** $\tau_{293}/\mu s^a$
1	*n*-Hexane	−0.11	0.31	0.1444 ± 0.0010	1.4465 ± 0.0109	1.3545 ± 0.0004
2	Diethyl ether	0.24	0.24	0.1754 ± 0.0013	1.6499 ± 0.0149	1.4438 ± 0.0150
3	Ethyl acetate	0.45	0.46	0.2675 ± 0.0023	2.1855 ± 0.0067	2.1673 ± 0.0128
4	Toluene	0.49	0.59	0.3031 ± 0.0037	2.5722 ± 0.0061	2.8108 ± 0.0340
5	Benzene	0.55	0.65	0.3145 ± 0.0021	2.5161 ± 0.0063	2.7391 ± 0.0308
6	Acetone	0.62	0.32	0.3001 ± 0.0050	2.3251 ± 0.0439	2.4325 ± 0.0092
7	Dichloromethane	0.73	0.44	0.4983 ± 0.0030	4.7714 ± 0.0381	4.7606 ± 0.0177
8	Glycerin triacetate (GTA)	0.63	23.00	0.7626 ± 0.0025	5.9599 ± 0.0491	8.7210 ± 0.1607
9	2,4-Dicyclohexyl-2-methyl pentane (DCMP)	0.14	38.7	0.4103 ± 0.0034	4.0531 ± 0.0298	6.2149 ± 0.0654
10	Dimethyl sulfoxide (DMSO)	1.00	2.24	0.6451 ± 0.0034	4.8613 ± 0.0121	n.d.^{b}

^{a}Average value of three experimental lifetimes. Error value was standard deviation of lifetime. ^{b}Not detected.

To gain a deeper understanding of the viscosity effect on isomerization of diradicals S-**DR4a** and S-**DR4b**, three highly viscous solvents DMSO, GTA and DCMP were used as medium to conduct the LFP experiments (Table 2.1, entries 8−10). Interestingly, the longest lifetimes were observed in GTA (entry 8) for both S-**DR4a** and S-**DR4b**, even though the $\pi*$ of GTA (0.63 kcal mol^{-1}) is considerably lower than that of DMSO (1.0 kcal mol^{-1}). Particularly, compared with the lifetimes obtained in acetone that has very similar polarity to GTA, the τ_{293} for S-**DR4a** and S-**DR4b** obtained in GTA are about 2.5-times longer. On the other hand, good linear correlations were not observed in the figures depicting the relationship between lifetime and polarity or viscosity (Figure 2.4). Meanwhile, comparing with the correlation coefficient obtained in seven low viscosity solvents (S-**DR4a**: 0.89; S-**DR4b**: 0.73), the coefficient values were found to be lower for both diradicals in correlation between the lifetime and polarity (S-**DR4a**: 0.57; S-**DR4b**: 0.43) in contrast the correlation between lifetime and viscosity were found to be better by the using of highly viscous solvents as medium. These results demonstrated that lifetime cannot be simply explained solely based on polarity changes and viscosity also have an important role in the isomerization of localized singlet diradicals. Besides, in Figure 2.4b, the correlation between the lifetime and viscosity for S-**DR4b** ($R^2 = 0.51$) was better than that for S-**DR4a** ($R^2 = 0.45$) which demonstrated that lifetime of S-**DR4b** is more sensitive to the changes in viscosity than that of S-**DR4a**. Notably, the slope values are almost same for S-**DR4a** and S-**DR4b** in Figure 2.4 (b), providing an evidence of alkoxy moiety remaining relative motionless in this isomerization process from the planar singlet diradicals having π-single bonding to the puckered ring-closing compounds.
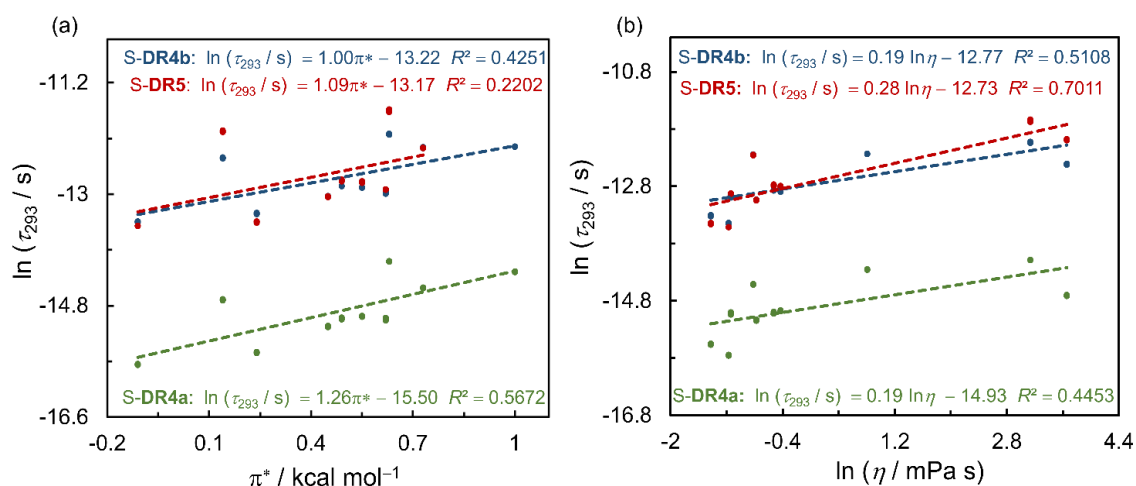
Figure 2.4. Correlations between the lifetimes (τ_{293}) of S-**DR4a** and S-**DR4b** with (a) polarity (π^*) and (b) viscosity (η) at 293 K in organic solvents (0.2 < η < 39 mPa s) (entries 1–10).

To further assess the influence of solvent viscosity and polarity on the lifetime of diradicals, LFP measurements of diradicals S-**DR4a** and S-**DR4b** were also conducted in binary systems containing organic solvent GTA/DMSO and ionic liquid [BMIM][PF$_6$] and the results are shown in Table 2.3. In order to measure the viscosity of binary systems, we assumed that the sum of the volumes of the pure components was equal to the total volume of the binary systems and calculated the density of binary mixtures for the measurement of viscosity. As clearly shown in Table 2.2, the predicted densities (ρ) are 1.27 and 1.14 g mL^{-1} (20 °C) when the DMSO mole fractions are 0.5953 and 0.9363, which reproduced well the previously experimental results at 25 °C (1.2752 and 1.1319 g mL^{-1}, DMSO mole fractions: 0.6001 and 0.9491).[36] Subsequently, the unknown viscosity of binary system was measured by Microviscometer Lovis 2000M at 20 °C (Table 2.2). To confirm the validity of viscosity, the viscosity of binary mixture where GTA mole fraction is 0.8474 was also detected and the value is 46.4 mPa s when density was 1 g mL^{-1} which is close to the value 48.15 mPa s when the density is 1.19 g mL^{-1}. Considering a wide range of viscosity (0.24 to 125.4 mPa s) used in present study, this slight experimentally error induced by density for viscosity is negligible in our research. Actually, the viscosity (57.35 mPa s) of [BMIM][PF$_6$] combined with DMSO (mole fraction: 0.3704) system obtained at 293

K was in fair similar with previously experimental value (56.306 mPa s, DMSO mole fraction: 0.4020) at 298.15 K.[37] Additionally, as expected, viscosity of binary systems increased with an increase in mole fractions of ionic liquid [BMIM][PF$_6$] for both two binary systems. We used the Kamlet−Abboud−Taft parameters $\pi*$ scale as empirical polarity parameter in present research because the better correlation of lifetime with the parameters $\pi*$ than $E_T(30)$ was observed.[15,31,32,38] The polarity $\pi*$ of binary systems was calculated according to Eq.5 where the wavelength of maximum absorption (λ_{max}) were obtained from the UV/Vis absorption spectra of 4-nitro-anisole in binary systems and the results are shown in Table 2.2. In contrast to the increase in polarity with a decrease in the GTA mole fraction, polarity decreased with a decrease in the DMSO mole fraction.

$$10^4/\lambda_{max} = 34.17 - 2.41\ \pi* \hspace{3cm} (5)$$

Table 2.2. η (20 °C) and $\pi*$ (23 °C) of the binary mixed systems of [BMIM][PF$_6$] + GTA/DMSO.

GTA mole fraction	λ_{max}/nm	$\pi*$/ kcal mol^{-1}	ρ/g mL^{-1} (calcd)[a]	η/mPa s
0	n.d.[b]	0.9[c]	n.c[d]	312[e]
0.3571	312.11	0.88	1.29	177.3
0.5263	311.73	0.87	1.26	125.4
0.6249	311.27	0.85	1.24	93.44
0.6896	310.70	0.82	1.23	81.13
0.8474	309.76	0.78	1.19	45.18
1	n.d.	0.63	1.16	23.00
DMSO mole fraction	λ_{max}/nm	$\pi*$/ kcal mol-1	ρ/g mL^{-1} (calcd)[a]	η/mPa s
0	n.d.	0.9	n.c.	312
0.1640	313.00	0.92	1.34	158.2
0.3704	313.21	0.93	1.32	57.35
0.5953	313.68	0.95	1.27	23.37
0.7463	314.25	0.97	1.23	10.84
0.9363	314.73	0.99	1.14	3.44
1	n.d.	1.00	1.10	2.24

[a]Calculated density. [b]Not detected. [c]The polarity of [BMIM][PF$_6$].[39] [d]Not calculated. [e]The viscosity of [BMIM][PF$_6$].[40]

Table 2.3. τ_{293} of the singlet diradicals S-**DR4a** and S-**DR4b** at 293 K in the binary systems of [BMIM][PF$_6$] + GTA/DMSO.

Entry	GTA molar fraction	π^*/kcal mol^{-1}	η/ mPa s	S-**DR4a** τ_{293}/μs^a	S-**DR4b** τ_{293}/μs^a
1	0.5263	0.87	125.4	1.5625 ± 0.0088	10.7003 ± 0.1059
2	0.6249	0.85	93.44	1.2927 ± 0.0025	9.3426 ± 0.0355
3	0.6896	0.82	81.13	1.2313 ± 0.0065	8.4704 ± 0.1442
4	0.8474	0.78	45.18	0.9968 ± 0.0126	7.1144 ± 0.0572
5	1	0.63	23.00	0.7626 ± 0.0025	5.9599 ± 0.0491
Entry	DMSO molar fraction	π^*/kcal mol^{-1}	η/ mPa s	S-**DR4a** τ_{293}/μs^a	S-**DR4b** τ_{293}/μs^a
6	0.3704	0.93	57.35	2.0775 ± 0.0270	15.0033 ± 0.1182
7	0.5953	0.95	23.37	1.4364 ± 0.0023	11.2203 ± 0.1547
8	0.7463	0.97	10.84	1.0022 ± 0.0007	7.8891 ± 0.0544
9	0.9363	0.99	3.44	0.6682 ± 0.0016	5.0925 ± 0.0994
10	1	1.00	2.24	0.6451 ± 0.0034	4.8613 ± 0.0121

^{a}Average value of three experimental lifetimes. Error value was standard deviation of lifetime.

The poor solubility of azoalkanes **AZ4a** and **AZ4b** hampered the measurement of lifetime of corresponding diradicals in solvents with more molar fraction of ionic liquid [BMIM][PF$_6$]. The longest lifetimes of S-**DR4a** and S-**DR4b** were obtained in DMSO+[BMIM][PF$_6$] system where the polarity and viscosity are 0.93 kcal mol^{-1} and 57.35 mPa s respectively (entry 6 in Table 2.3), and the lifetime values are approximately 3 times longer than those in pure DMSO (entry 10 in Table 2.3) with slightly decreased polarity (1 kcal mol^{-1}) and remarkable lower viscosity (2.24 mPa s). For GTA+[BMIM][PF$_6$] system, the expected trends were observed for diradicals S-**DR4a** and S-**DR4b** that lifetimes increased as the solvents polarity and viscosity increasing. Whereas lifetimes increase with the increasing viscosity and decreasing polarity for diradicals S-**DR4a** and S-**DR4b** in DMSO and [BMIM][PF$_6$] mixed system. The experimental evidence presented above appreciably suggests that the solvent viscosity act more effectively to afford increased lifetimes of S-**DR4a** and S-**DR4b** in

highly viscous solvents. In other words, the viscosity effect controls isomerization of planar localized singlet diradicals featuring π-single bonding character to σ-single bonding species with puckered structure in highly viscous solvents. It is noteworthy that although viscosities are almost same for the binary mixture (entry 7 in Table 2.3; DMSO mole fraction: 0.5953) and pure GTA (entry 5 in Table 2.3), the lifetimes values in binary mixture are about 2-fold than those in pure GTA for S-**DR4a** and S-**DR4b**. The results disclose a very fact that polarity also plays an important role in isomerization of diradicals in highly viscous solvents. For the same reason, the shorter lifetimes of S-**DR4a** and S-**DR4b** obtained in GTA system with the GTA molar fraction 0.5263 (entry 1 in Table 2.3) relative to DMSO system with the DMSO molar fraction 0.3704 (entry 6 in Table 2.3) resulted from the impressively lower polarity.

To quantify the relationship between lifetime and polarity and viscosity, we sought to employ linear regression analysis on 18 sets of data for S-**DR4a** and S-**DR4b** (Table 2.1, pure solvents and Table 2.3, binary systems) according to Eq.6 where A, B and C are polarity, viscosity coefficients and a constant term, respectively. All the terms are compound-dependent and the results are summarized in Table 2.4.

$$\ln(\tau_{293}) = A\pi* + B\eta + C \qquad (6)$$

In this case, the ratios between B and A (S-**DR4a**: 0.0062, S-**DR4b**: 0.0065) were calculated and negligible difference in these two ratios is considered as an indication of aforementioned conclusion, namely, alkoxy group does not change its relative position during isomerization process from diradicals having planar structure to *trans* ring-closing compounds featuring puckered structure. In addition, lifetimes for diradicals in gas phase ($A = 0$, $B = 0$) at 293 K were calculated to be 0.15 μs (S-**DR4a**) and 1.50 μs (S-**DR4b**) and those values are in accordance with the results obtained in *n*-hexane (Table 2.1, entry 1). To this end, in the light of Eq 6., the relationships between predicated and experimental $\ln(\tau_{293})$ are shown in Figure 2.5 and the validation of regression analysis was proved by good agreements where most data points were near the equivalence line.

Table 2.4. Regression analysis for fitting the observed ln (τ_{293}) to Eq. (6) for S-**DR4a** and S-**DR4b** in 18 sets of solvents including pure organic solvents and binary systems solvents.

Coefficient	S-**DR4a**	S-**DR4b**
A	1.6273	1.3753
B	0.0101	0.0089
C	−15.6907	−13.4097
B/A	0.0062	0.0065
τ_{293} / μs (A = 0, B = 0)	0.15	1.50
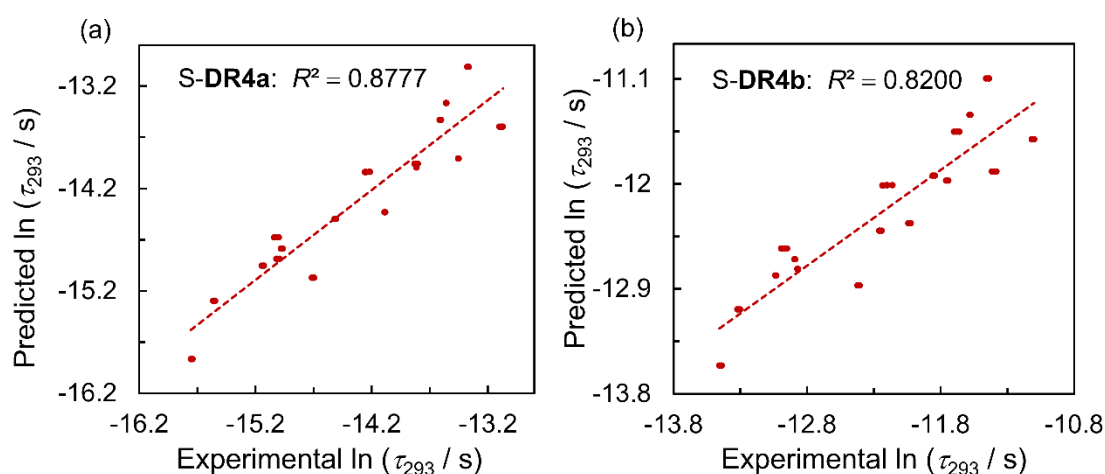
Figure 2.5. Correlation between the experimental and predicted ln (τ_{293}) for (a) S-**DR4a** and (b) S-**DR4b** in 18 sets of solvents including pure organic solvents and binary systems solvents.

2.4 The molecular motion during the isomerization reaction

As mentioned previously, alkoxy group does not change its relative position during isomerization process from planar localized singlet diradicals featuring π-single bonding to σ-single bonding species with puckered structure which promoted us to put forward a hypothesis that the relative mobility moiety is cyclopentane moiety instead of alkoxy group. Inspired by this, S-**DR5** with long carbon chain at remote position from the reactive center was designed and performed similar LFP experiments in organic solvents (Table 2.1). The poor solubility of corresponding azoalkane

AZ5 in DMSO and binary systems precluded the measurement of lifetime of S-**DR5** in DMSO and binary systems.

Lifetimes of S-**DR4s** and S-**DR5** in low viscous solvents ($\eta < 1$ mPa s) were very similar (entry 1–7, Table 2.1) benefiting from the similar steric hindrance between the alkoxy group and phenyl ring in corresponding transition states. Surprisingly, the lifetimes of S-**DR3** are significantly elongated in highly viscous solvents GTA and DCMP which were about 1.5 times longer than those of S-**DR4b**. On the basis of the fact that the transition state theory cannot be applied in high-viscosity solvents and observed rate constant was determined by solvent fluctuation, hence, the strongly influenced by viscosity for S-**DR5** supports aforementioned hypothesis that the relative mobility molecular moiety is cyclopentene part during isomerization in solvents. This becomes especially clearly shown from the plots of viscosity dependence (Figure 2.4b). Different from nearly equal values of slope for S-**DR4a** and S-**DR4b**, slope for S-**DR5** is remarkable larger than that for S-**DR4b**.

Aiming at further understanding of polarity and viscosity roles in the correlation between lifetime, we performed a regression analysis using all the data acquired in organic solvents for S-**DR4a**, S-**DR4b** and S-**DR5** according to Eq. 6 (Table 2.5). The ratio between B and A for S-**DR5** (0.0264) is larger than that for S-**DR4a** (0.0167) and S-**DR4b** (0.0205) suggested the most pronounced viscosity effects for S-**DR5**. Moreover, based on regression analysis, lifetimes of three diradicals in gas phase ($A = 0$, $B = 0$) at 293 K were also predicted and those are 0.14 μs (S-**DR4a**), 1.38 μs (S-**DR4b**) and 1.25 μs (S-**DR5**) which are consistent with those measured in n-hexane (Table 2.1: 0.14, 1.45 and 1.36 μs). The validation of regression analysis was also confirmed by good quality fitting of experimental and predicated ln (τ_{293}) (Figure 2.6).

Table 2.5. Regression analysis for fitting the observed ln (τ_{293}) to Eq (6) for S-**DR4a**, S-**DR4b**, and S-**DR5** in pure organic solvents.

Coefficient	S-**DR4a**	S-**DR4b**	S-**DR5**
A	1.4812	1.2265	1.4518
B	0.0248	0.0252	0.0384
C	-15.7681	-13.4965	-13.5919
B / A	0.0167	0.0205	0.0264
τ_{293} / μs (A = 0, B = 0)	0.14	1.38	1.25
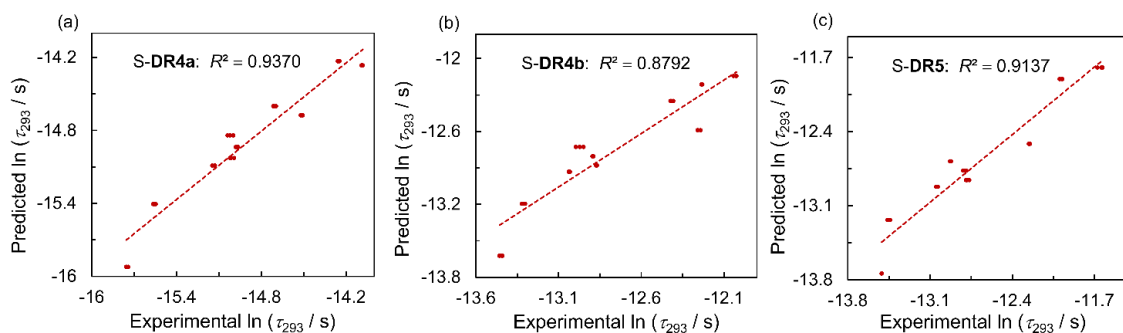
Figure 2.6. Correlation between the experimental and predicted ln (τ_{293}) for (a) S-**DR4a**, (b) S-**DR4b** and (c) S-**DR5** in pure organic solvents.

2.5　Summary of this chapter

In conclusion, the lifetimes of localized singlet diradicals corresponding isomerization from diradicals featuring π-single bonding to ring-closed compounds with σ-single bonding have been measured in 18 different solvents and solvent mixtures with broadly ranges of polarity and viscosity. Following the previous results in earlier studies, an increase in solvent polarity or viscosity leads to increase in the lifetimes of diradicals. Apart from that, better linear dependence of lifetime on π* of S-**DR4a** and S-**DR4b** were obtained in low viscous solvents ($\eta < 1$ mPa s). Notably, in high viscous solvents, specifically in binary systems containing organic solvent

GTA/DMSO and ionic liquid [BMIM][PF$_6$], lifetimes were strongly affected by viscosity. The different sensitivity on viscosity for S-**DR4b** and S-**DR5** in pure organic solvents elucidated the relative mobility of cyclopentene moiety in isomerization from planar diradicals to puckered σ-single bonding species. Reasonable regression analysis makes us assess the polarity and viscosity effects on the lifetime of diradicals quantificationally. The present study not only provides deeper insight into the character of singlet diradicals but also furnishes a demonstrative example that viscosity effect serves as a promising strategy to explore dynamic routes of the reactant molecules for isomerization in solvents.

2.6   Experimental section

All reagents that were purchased from TCI, Wako, Sigma Aldrich and Kanto were used directly without further purification. A Bruker Ascend 400 (^{1}H NMR: 400 MHz, ^{13}C NMR: 100 MHz) spectrometer was used to detect NMR spectra at 298 K and the position of peaks was referenced to the residual solvent peak. Coupling constants (J) are represent by Hz and chemical shifts (δ) in ppm. The resonance multiplicities singlet, doublet, triplet and multiplet are expressed by the abbreviations s, d, t, and m, respectively. Mass spectrometric data were acquired from the Thermo Fisher Scientific LTQ Orbitrap XL and JMS-T100GCV AccuTOF GCv. A SHIMADZU UV-3600 Plus spectrometer was used for the measurement of UV/Vis spectra with a slit width of 1 and 0.01 nm. Sub-microsecond laser flash photolysis (LFP) for photodenitrogenation of diradicals were performed by the excitation source with a tunable Nd:YAG minilite laser at 355 nm. A 150 W xenon arc lamp as light source, a photomultiplier and a Unisoku MD200 monochromator detection compose the monitoring system. The temperature was governed by Unisoku CoolSpek USP-203-B. A passive Q-SWITCH microchip laser at 355 nm was excitation source for LFP system.
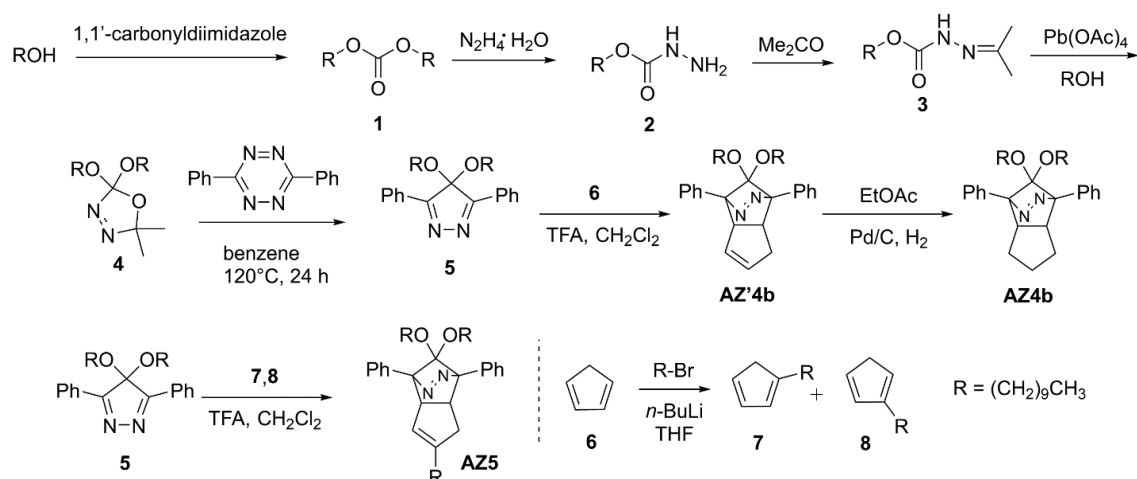
Scheme S2.1. Synthesis of azoalkanes **AZ4b** and **AZ5**.

Didecyl carbonate **1**: 1,1'-carbonyldiimidazole (4.00 g, 24.68 mmol, 1 equiv) and 1-decanol (19 mL, 4 equiv) was added into a flask at room temperature under a nitrogen atmosphere. The mixture was stirred for 22 h at 55 °C (oil bath) and quenched with saturated brine, extracted with EtOAc. Dry the combined organic layers with Na_2SO_4, filter and concentrate resulting in crude. The crude was used directly for the next step. APCI-MS calculated for $C_{21}H_{43}O_3$ [M+H]$^+$ = 343.32067, found 343.32080.

Decyl hydrazinocarboxylate **2**: Under a nitrogen atmosphere, crude didecyl carbonate **1** and hydrazine hydrate (1.64 mL, 1.5 equiv) was added into a flask and stirred for 1 h at room temperature and then heated the reaction to 80 °C (oil bath). After 20 h, cool the reaction mixture to room temperature and wash it by aq $NaHCO_3$ and H_2O. After extracted (EtOAc), dried (Na_2SO_4), filtered and evaporated, the crude was purified by column chromatography on silica gel (hexane : EtOAc = 1 : 1) affording white solid compound decyl hydrazinocarboxylate **2** (4.20 g, 19.41 mmol, 78.7 % of 2 steps). ^{1} **H NMR** (400 MHz, CDCl$_3$): δ = 5.88 (s, 1H), 4.10 (t, J = 6.75 Hz, 2H), 3.73 (d, J = 3.35 Hz, 2H), 1.65−1.58 (m, 2H), 1.36−1.21 (m, 14H), 0.88 (t, J = 7.00 Hz, 3H).

3: A flask was charged with mixture of decyl hydrazinocarboxylate **2** (0.82 g, 3.78 mmol) and Na_2SO_4 (0.81 g, 1.5 equiv). The mixture was stirred at room temperature under a nitrogen atmosphere in acetone (7 mL) for overnight, subsequently filtered and concentrated to yield compound **3** as orange solid (0.96 g, 3.74 mmol), which was directly used for next step.

4: Lead tetraacetate (2.00 g, 1.2 equiv), 1-decanol (2.2 mL, 3.1 equiv) and CH_2Cl_2 (1.6 mL) were added into a two-neck flask under a nitrogen atmosphere. Then **3** (0.96 g, 3.74 mmol) dissolved in CH_2Cl_2 (3.8 mL) was added into flask dropwise at 0 °C. Stir the reaction mixture at 0 °C for 2 h and follow additional 24 h stirring at room temperature. Next, add aq $NaHCO_3$ into the flask and stir resulting mixture for 20 min. Then, filter the mixture using a pad of celite and wash the solution by aq $NaHCO_3$, brine and extract with EtOAc. Solvent was evaporated and the crude was purified by column chromatography on silica gel (hexane : EtOAc = 10 : 1) leading to **4**, which was used for next step directly. HRMS (EI) calculated for $C_{24}H_{49}N_2O_3$ $[M+H]^+ = 413.3743$, found 413.3725.

5: Dissolve **4** (0.63 g, 1.53 mmol) in benzene (4 mL) and mix with 3,6-diphenyl-1,2,4,5-tetrazine (0.40 g, 1.1 equiv) in a sealed pressure tube. The mixture stirred at 120 °C (oil bath) for 24 h. After evaporation and purification by column chromatography on silica gel (hexane : EtOAc = 20 : 1), **5** (0.37 g, 0.70 mmol, 19 % of 3 steps) was obtained as yellow oil. **^{1} H NMR** (400 MHz, $CDCl_3$): δ = 8.31−8.28 (m, 4H), 7.57−7.47 (m, 6H), 3.09 (t, J = 6.34 Hz, 4H), 1.47−1.39 (m, 4H), 1.31−0.96 (m, 28H), 0.87 (t, J = 6.85 Hz, 6H). ESI-MS calculated for $C_{35}H_{53}N_2O_2$ $[M+H]^+ = 533.41016$, found 533.40961.

7 and **8**: A flask was charged with a solution of cyclopentadiene **6** (3.3 mL, 2 equiv) in THF, followed by the addition of a 2.3 M solution of *n*-BuLi in hexane (13.0 mL, 1.5 equiv) slowly at −78 °C under a nitrogen atmosphere. The reaction mixture was stirred at −78 °C for 1 h. Then add 1-bromodecane dropwise at −78 °C and stir the mixture for additional 65 h at room temperature. Next, the reaction was quench by ice water and then add saturated NH_4Cl into the mixture. After washing (brine), extraction (EtOAc), drying (Na_2SO_4), filtration, evaporation of solvent, the residue was purified by column chromatography on silica gel using hexane only to produce **7** and **8** and the mixture product was directly used for next step. APCI-MS calculated for $C_{15}H_{27}$ $[M+H]^+ = 207.21073$, found 207.21069.

AZ'4b: A flask was charged with a solution of cyclopentadiene (0.58 mL, 10 equiv), **5** (0.38 g, 0.71 mmol) and CH_2Cl_2 (2 mL). Trifluoroacetic acid (10.5 μL, 0.2 equiv) was added dropwise at 0 °C under a nitrogen atmosphere in the absence of light. After stirring for 2 h, quench the reaction by aq $NaHCO_3$, wash the organic layer by brine and extract with CH_2Cl_2.

Next, after dry, filtration, concentration, and purification via column chromatography on silica gel (hexane : EtOAc = 10 : 1), **AZ'4b** (0.25 g, 0.42 mmol, 59 %) was prepared as colourless oil. [1] **H NMR** (400 MHz, CDCl$_3$): δ = 8.00–7.88 (m, 4H), 7.48–7.35 (m, 6H), 5.59–5.50 (m, 2H), 4.18–4.12 (m, 1H), 3.73–3.66 (m, 1H), 3.10–3.04 (m, 2H), 2.84–2.73 (m, 2H), 2.39–2.20 (m, 2H), 1.48–0.97 (m, 32H), 0.88 (m, 6H).

AZ4b: The [4+2] cycloadduct **AZ'4b** (0.25 g, 0.42 mmol) was dissolved in EtOAc (4 mL) and palladium (0.05 g, 1.1 equiv) on activated carbon 10 % was added into the mixture under a hydrogen gas atmosphere in absence of light. After stirring 37 h at room temperature, filtration over celite, concentration and purification via column chromatography and recycle column chromatography on silica gel, target compound **AZ4b** was achieved (0.19 g, 0.32 mmol, 74 %) as colourless oil (hexane : EtOAc = 10 : 1). [1] **H NMR** (400 MHz, CDCl$_3$): δ = 7.96–7.91 (m, 4H), 7.46–7.35 (m, 6H), 3.58–3.51 (m, 2H), 3.04 (t, J = 6.36 Hz, 2H), 2.76 (t, J = 6.32 Hz, 2H), 1.66–1.37 (m, 6H), 1.33–0.96 (m, 32H), 0.88 (m, 6H).

AZ5 was synthesized according to the procedure of synthesis for **AZ'4b**. The structure of compound **AZ5** was confirmed by NOESY NMR spectrum. [1] **H NMR** (400 MHz, CDCl$_3$): δ = 8.00–7.88 (m, 4H), 7.47–7.35 (m, 6H), 5.14 (s, 1H), 4.13–4.07 (m, 1H), 3.74–3.66 (m, 1H), 3.10–3.01 (m, 2H), 2.84–2.73 (m, 2H), 2.31–2.10 (m, 2H), 1.90–1.80 (m, 2H), 1.47–0.96 (m, 48H), 0.92–0.84 (m, 9H). [13] **C NMR** (100 MHz, CDCl$_3$): δ = 149.03, 137.08, 136.80, 128.86, 128.36, 128.13, 127.95, 127.73, 119.52, 117.92, 94.75, 93.07, 64.19, 63.91, 57.46, 43.14, 34.82, 32.06, 31.15, 30.02, 29.70, 29.48, 29.35, 27.59, 26.37, 25.95, 22.83, 14.26.
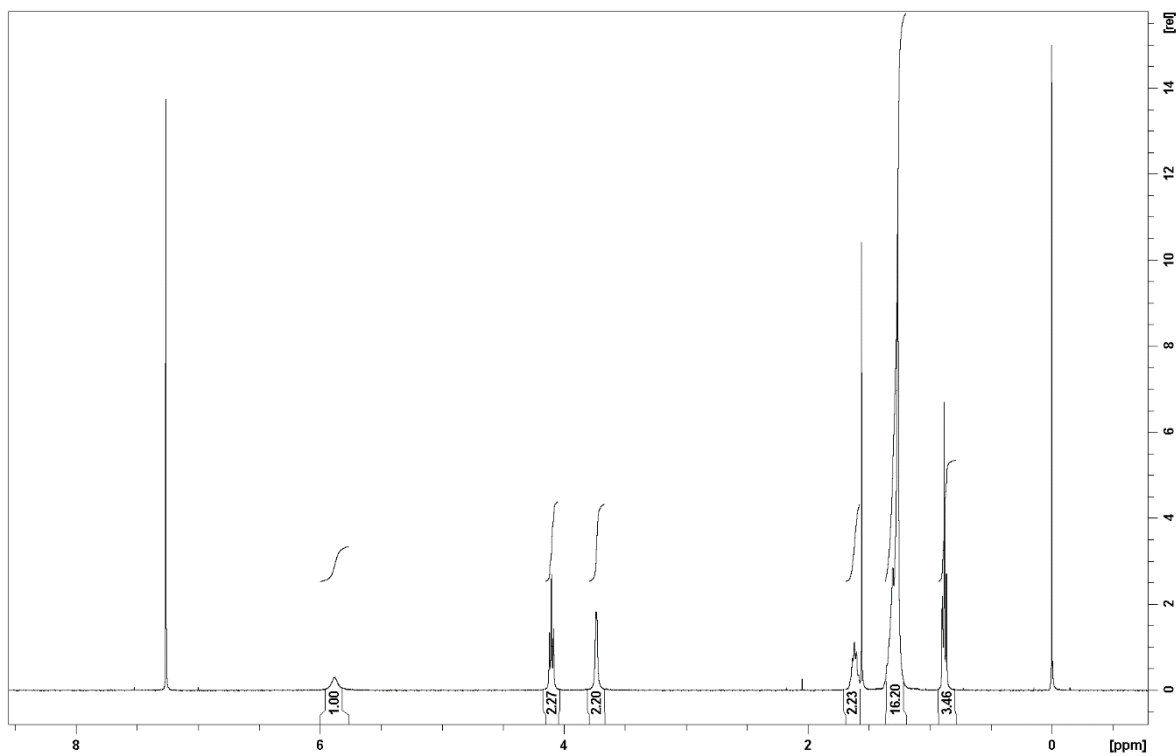
Figure S2.1. ^{1}H NMR spectrum of **2** (CDCl$_3$, 400 MHz).
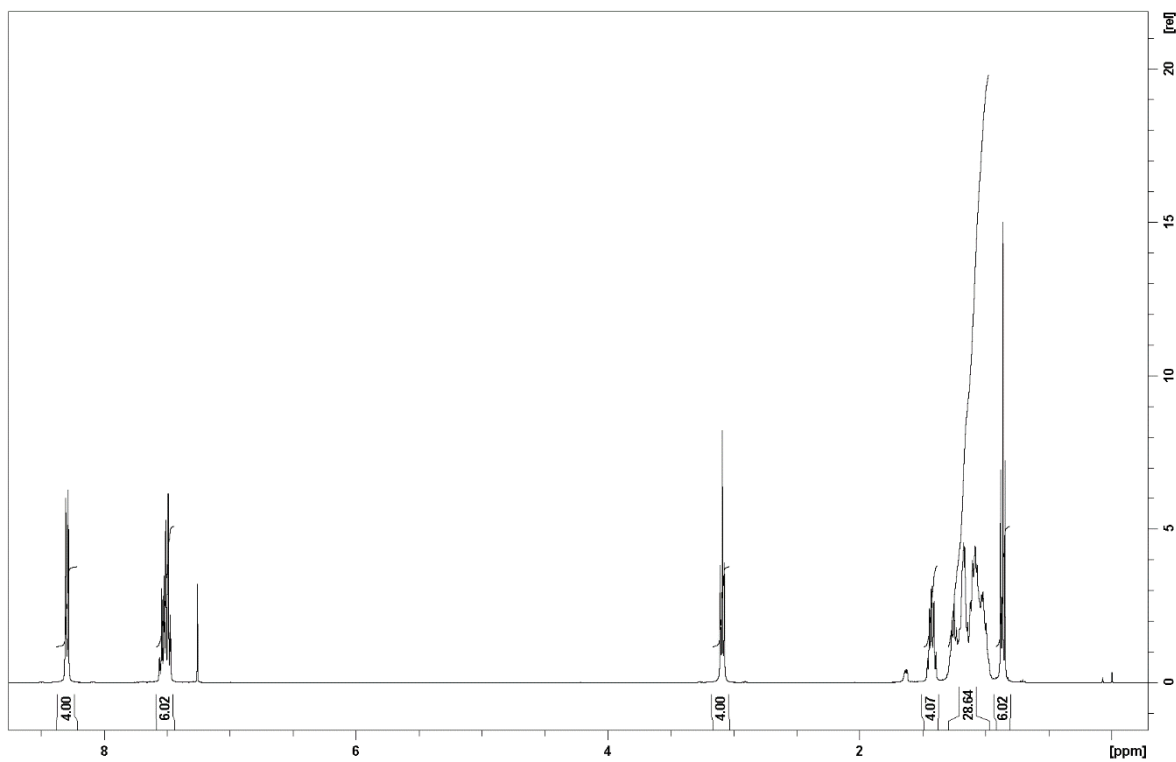
Figure S2.2. ^{1}H NMR spectrum of **5** (CDCl$_3$, 400 MHz).
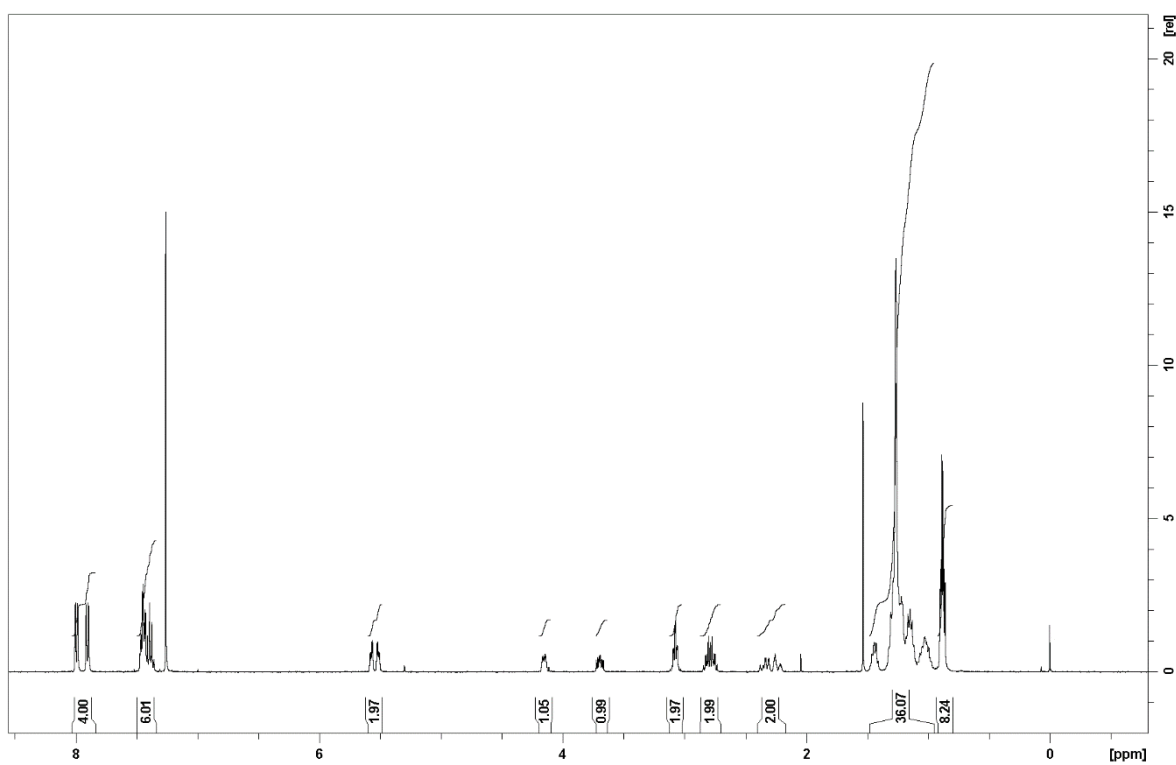
Figure S2.3. ^{1}H NMR spectrum of **AZ'4b** (CDCl$_3$, 400 MHz).
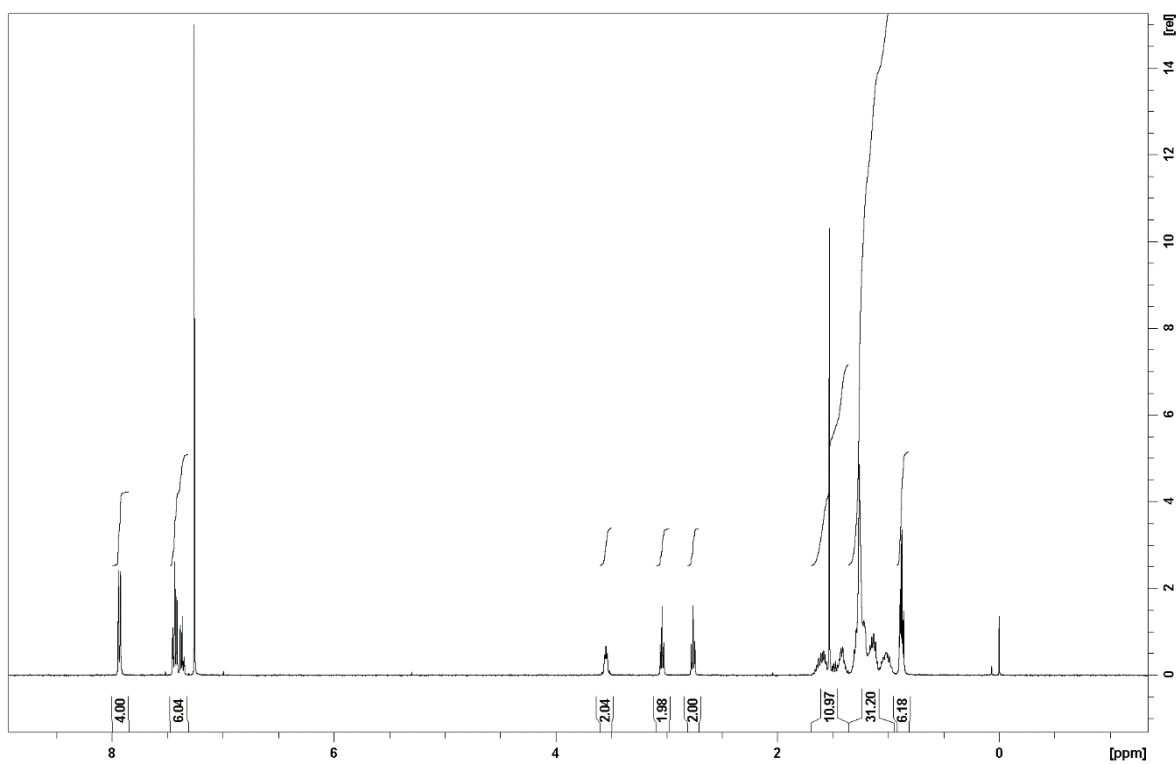
Figure S2.4. ^{1}H NMR spectrum of **AZ4b** (CDCl$_3$, 400 MHz).
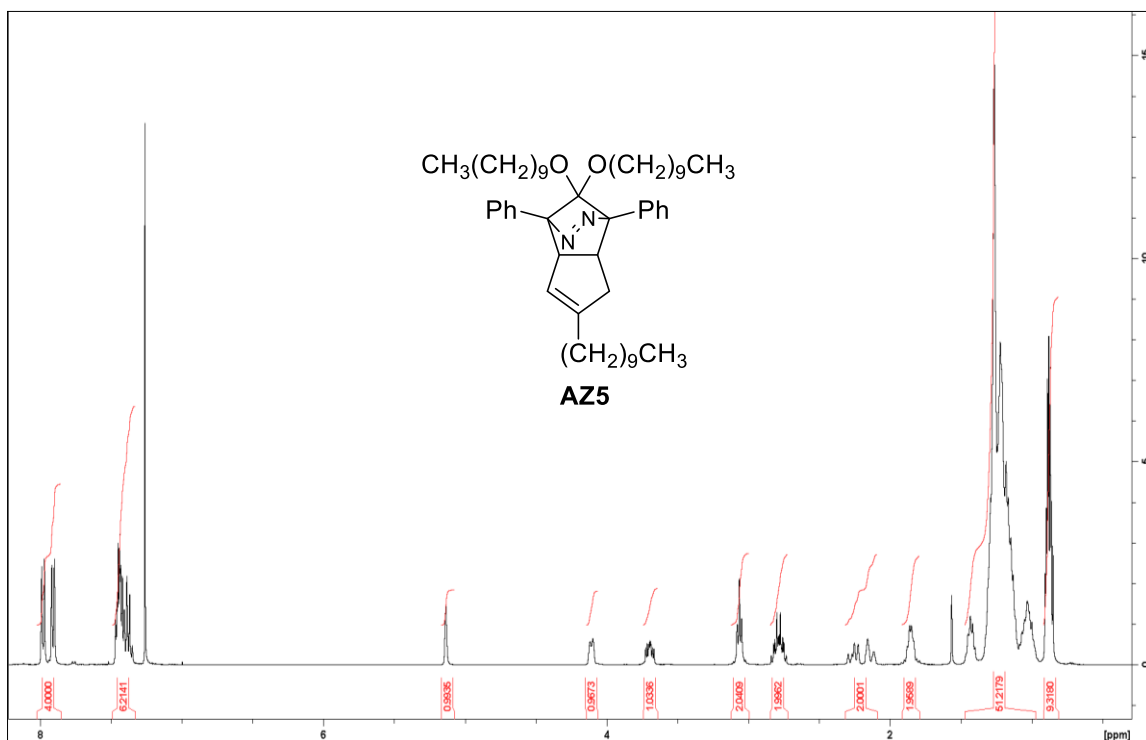
Figure S2.5. ^{1}H NMR spectrum of **AZ5** (CDCl$_3$, 400 MHz).
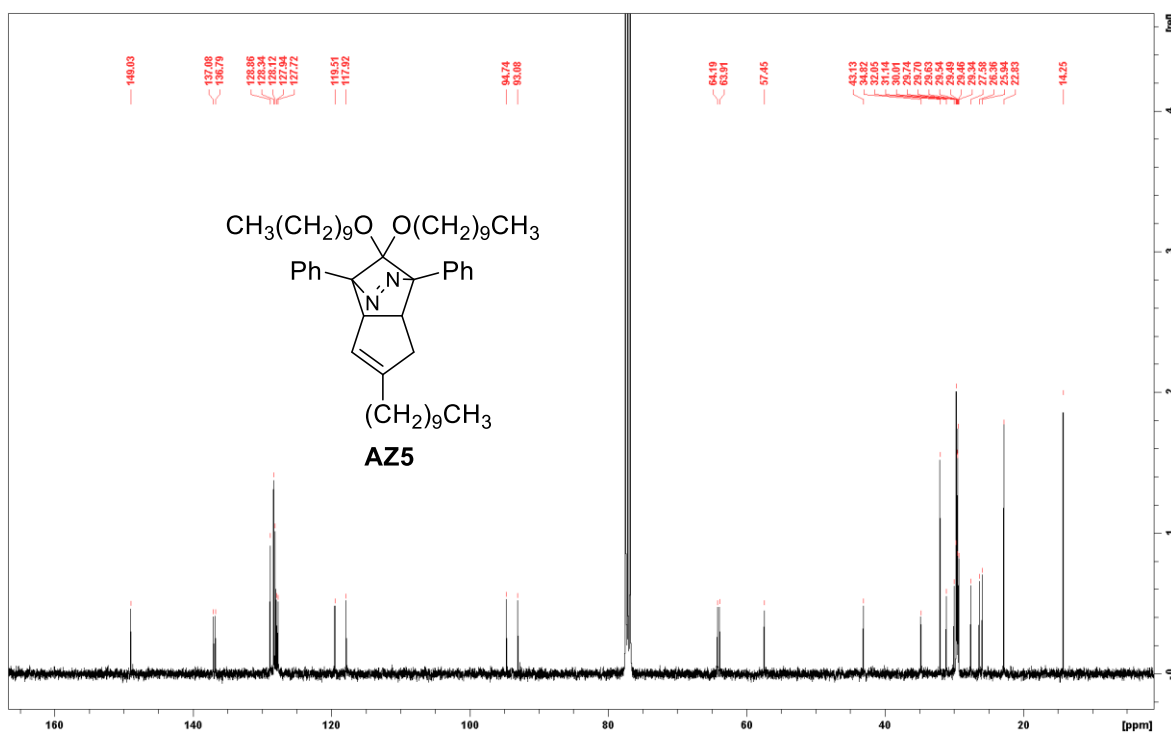
Figure S2.6. ^{13}C {^{1}H} NMR spectrum (CDCl$_3$, 400 MHz).
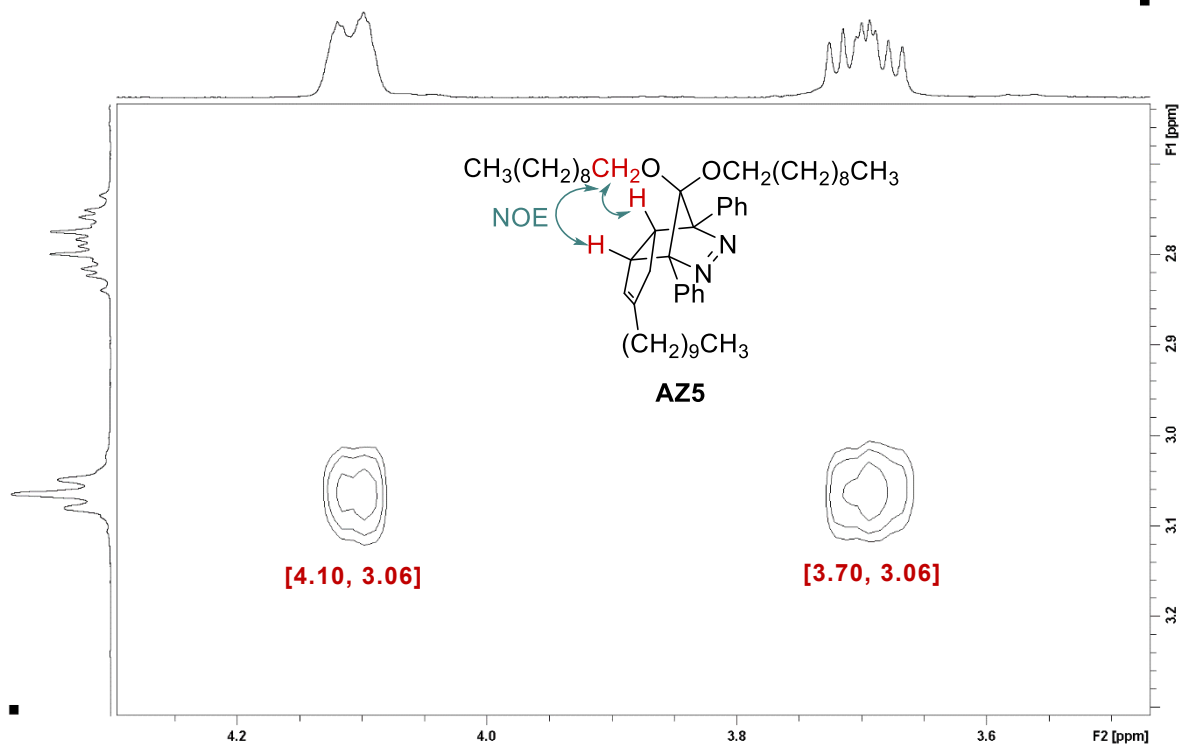
Figure S2.7. 2D NOESY NMR spectrum of **AZ5** (CDCl$_3$, 400 MHz).
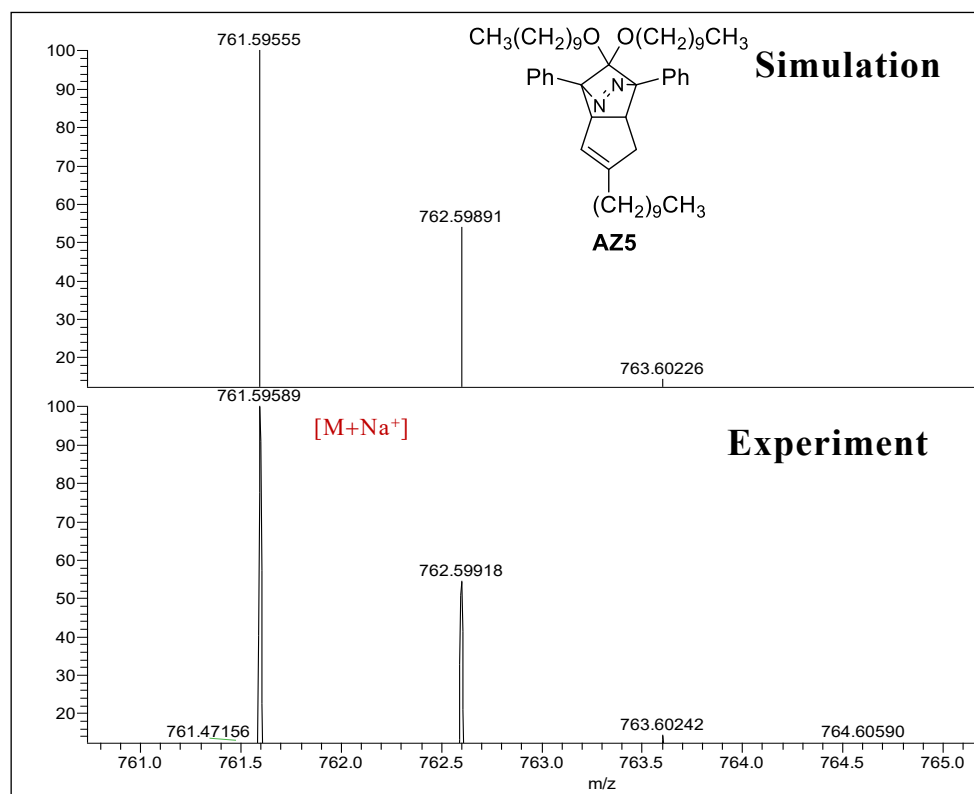
Figure S2.8. High resolution mass spectrum (ESI) of **AZ5**.
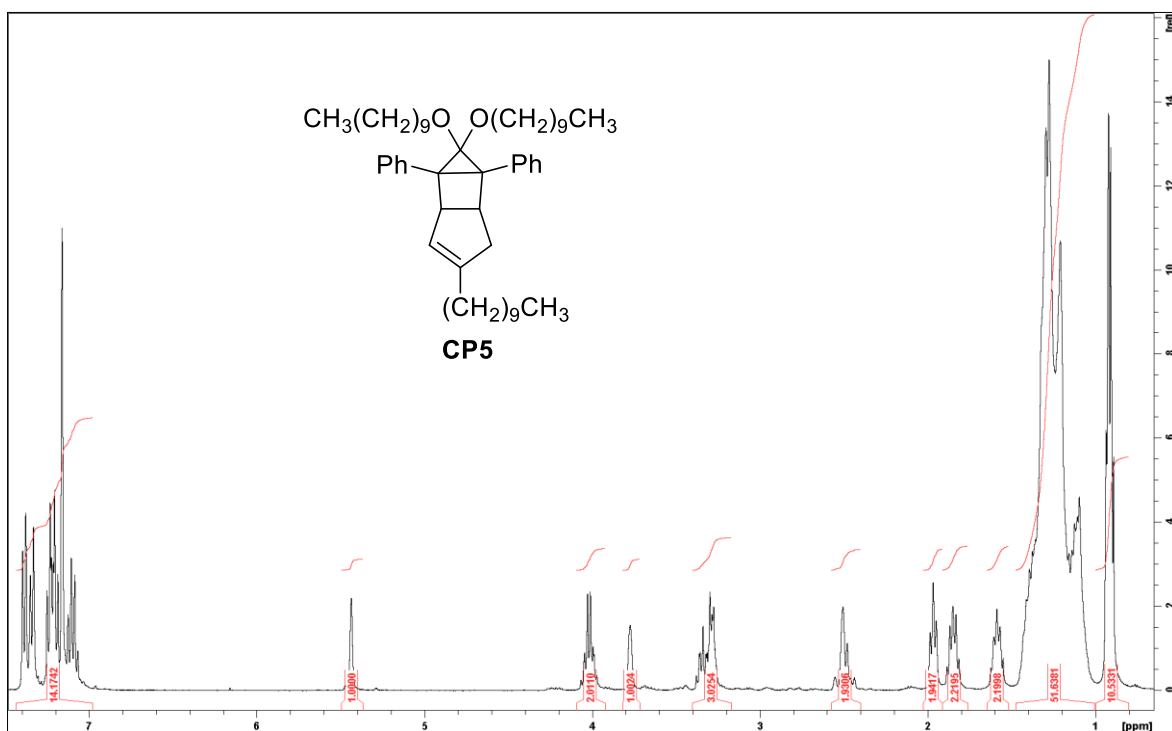
Figure S2.9. ^{1}H NMR spectrum of **CP5** (C$_6$D$_6$, 400 MHz).
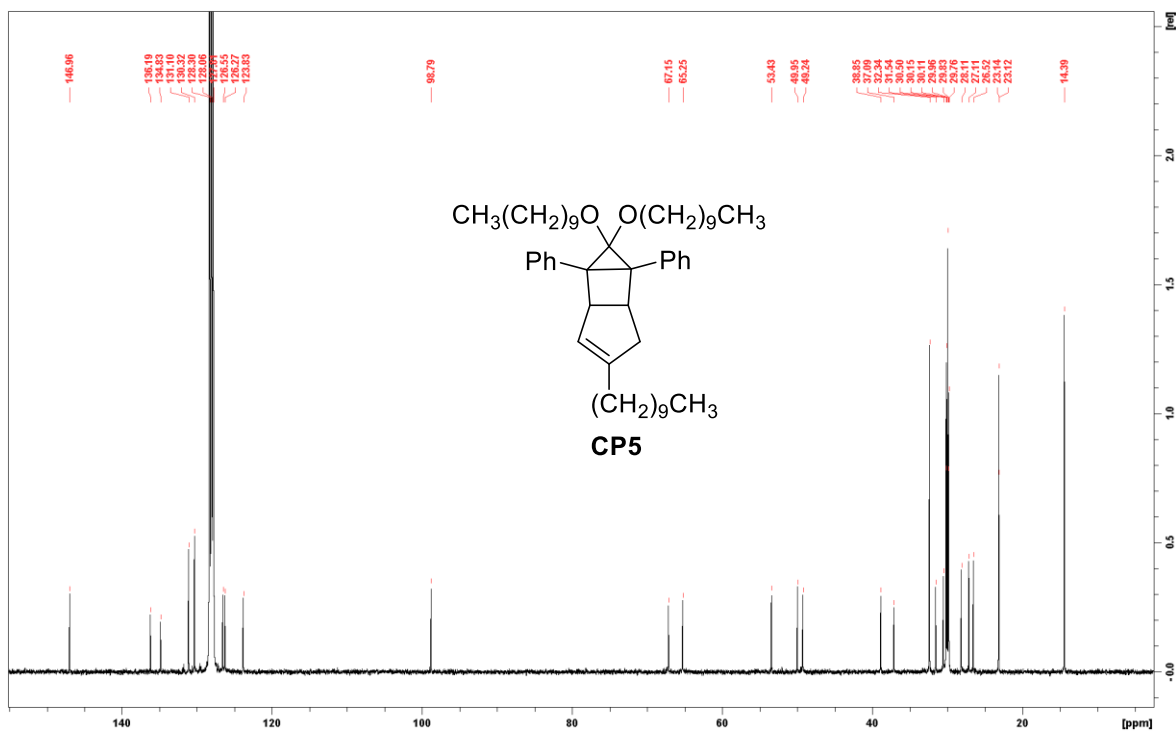
Figure S2.10. ^{13}C {^{1}H} NMR spectrum of **CP5** (C$_6$D$_6$, 100 MHz).
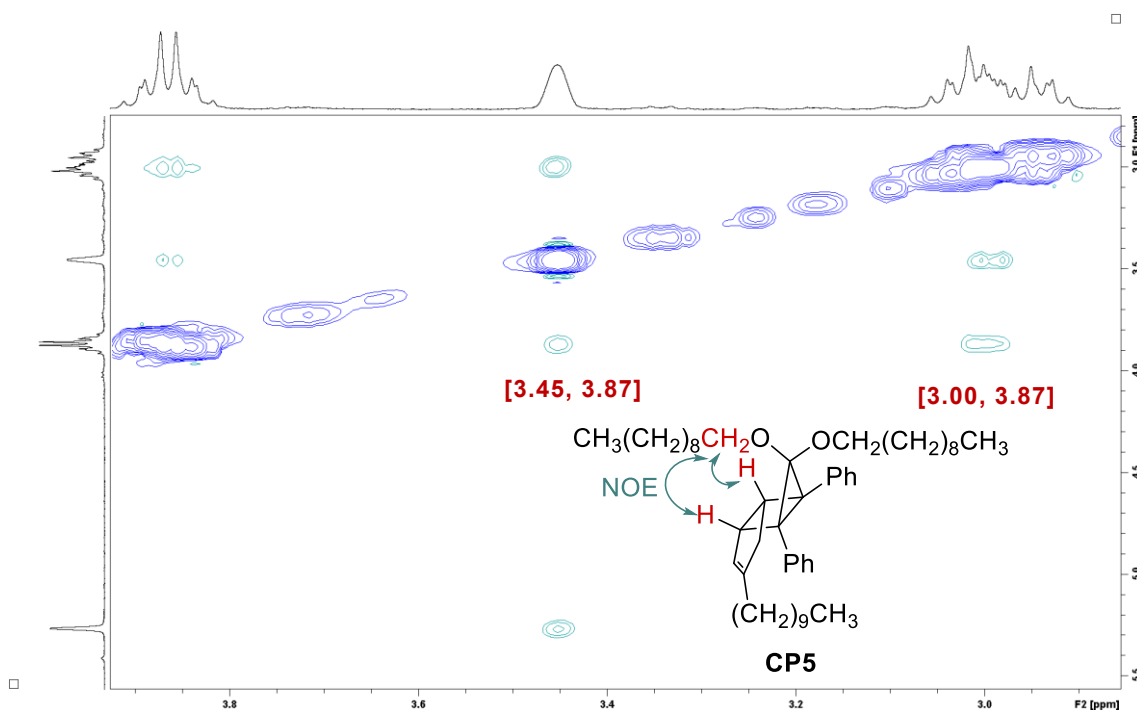
Figure S2.11. 2D NOESY NMR spectrum of **CP5** (CDCl$_3$, 400 MHz).
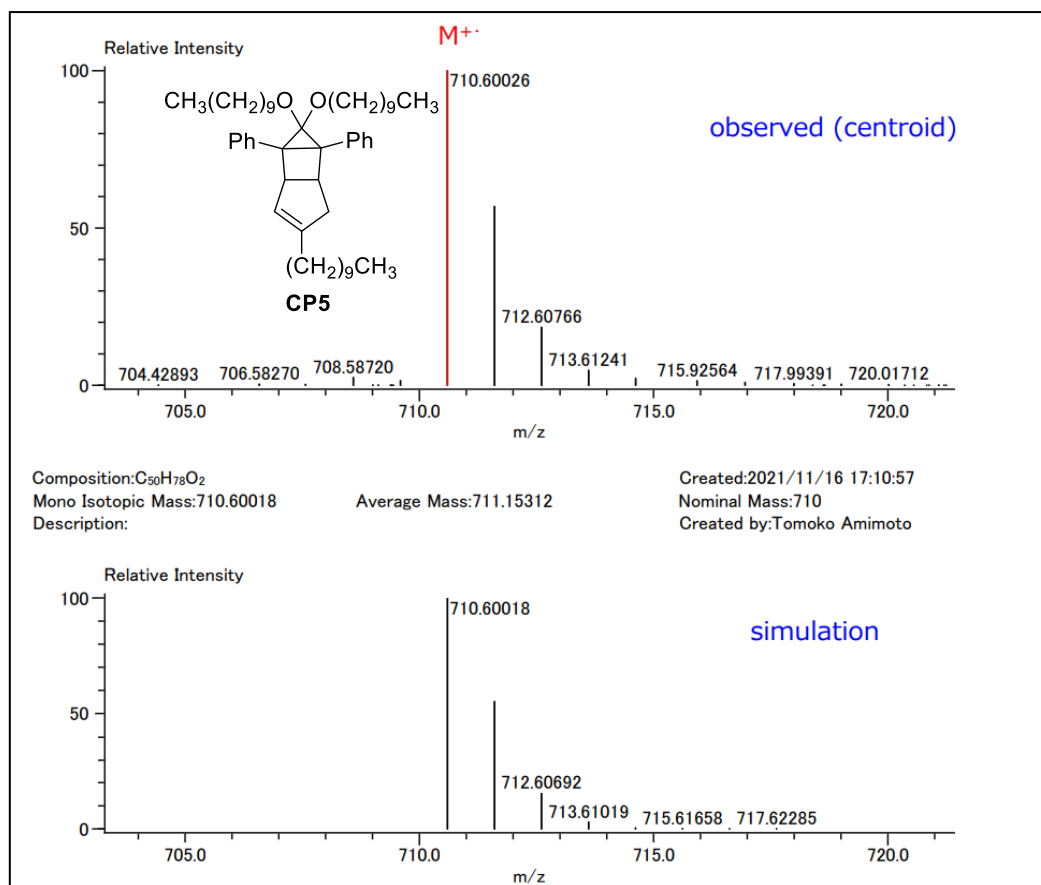
Figure S2.12. High resolution mass spectrum (FD) of **CP5**.

Determination of polarity

Table S2.1. Determination of polarity (π^*) of binary systems containing 1-Butyl-3-methylimidazolium hexafluorophosphate ([BMIM][PF$_6$]) and glycerin triacetate (GTA)/ dimethyl sulfoxide (DMSO).

Entry	GTA mole fraction	$\lambda_{\max}$ / nm	π^* / kcal mol^{-1}
1	0.3571	312.11	0.88
2	0.5263	311.73	0.87
3	0.6249	311.27	0.85
4	0.6896	310.70	0.82
5	0.8474	309.76	0.78
Entry	DMSO mole fraction	$\lambda_{\max}$ / nm	π^* / kcal mol^{-1}
6	0.1640	313.00	0.92
7	0.3704	313.21	0.93
8	0.5953	313.68	0.95
9	0.7463	314.25	0.97
10	0.9363	314.73	0.99
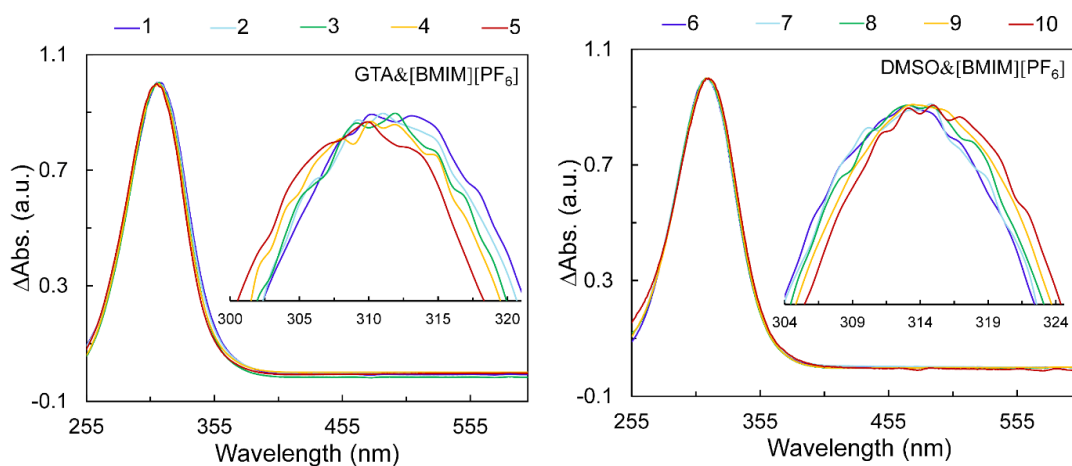
Figure S2.13. UV-vis absorption spectra of 4-nitroanisole in binary systems containing [BMIM][PF$_6$] and GTA/DMSO (inset: UV-vis absorption spectra with a step of 0.01 nm) (Table S2.1: entries 1−10).
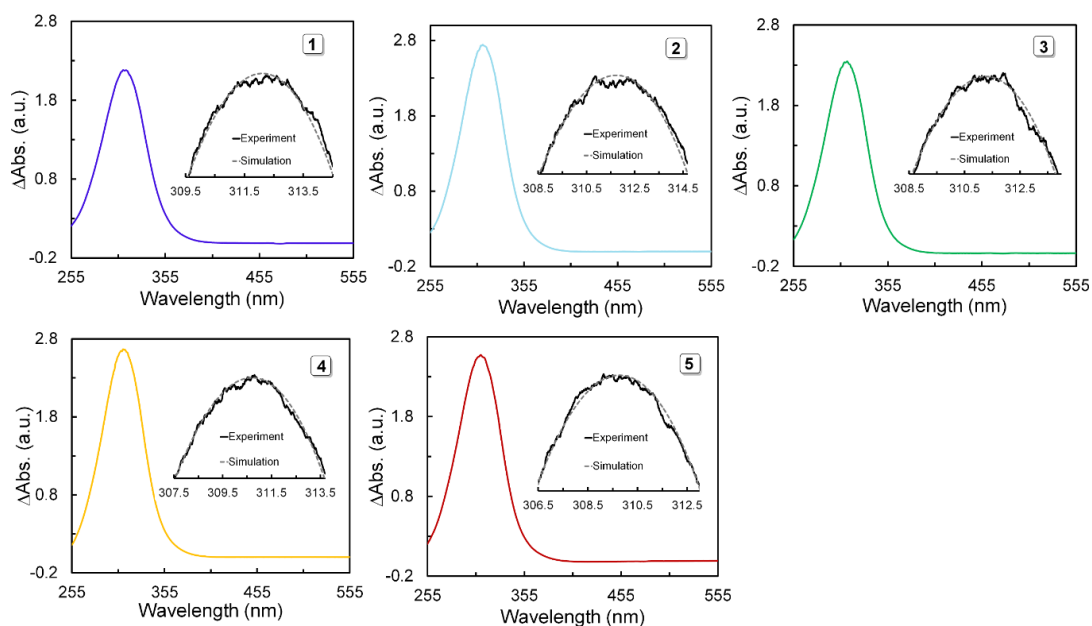
Figure S2.14 UV-vis absorption spectra of 4-nitroanisole in binary systems containing [BMIM][PF$_6$] and GTA (inset: experimental and simulated UV-vis absorption spectra with a step of 0.01 nm) (Table S2.1: entries 1−5).
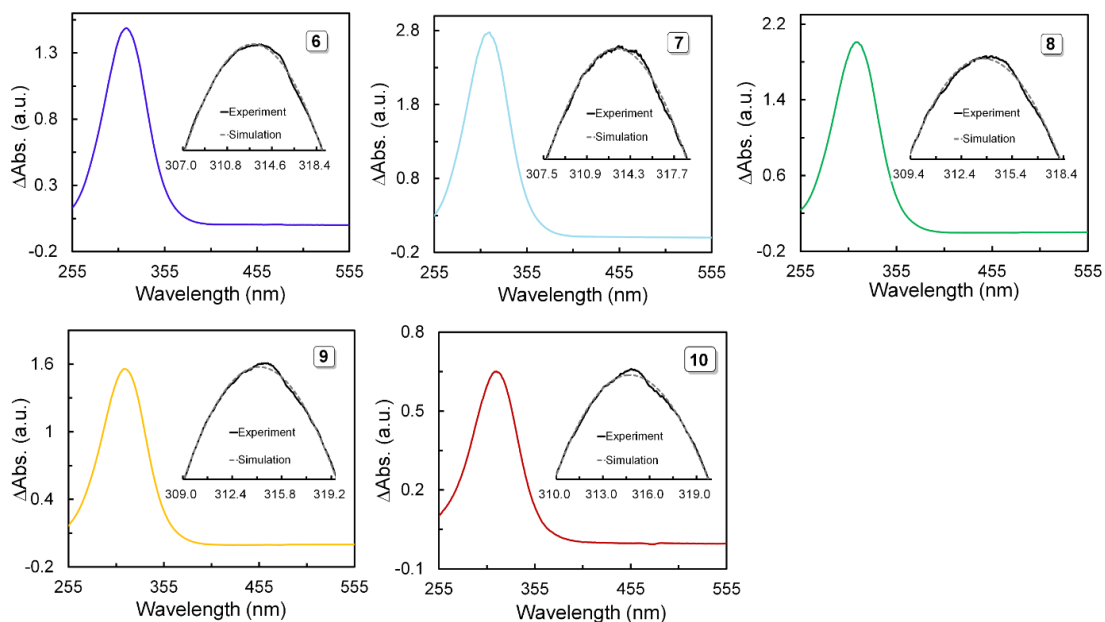

Figure S2.15 UV-vis absorption spectra of 4-nitroanisole in binary systems containing [BMIM][PF$_6$] and DMSO (inset: experimental and simulated UV-vis absorption spectra with a step of 0.01 nm) (Table S2.1: entries 6−10).

Table S2.2. Equation for simulated UV-vis absorption spectra.

Entry	GTA mole fraction	Equation	R^2
1	0.3571	$y = 2.77\text{E-08}x^6 - 5.13\text{E-05}x^5 + 3.96\text{E-02}x^4 - 1.63\text{E+01}x^3 + 3.77\text{E+03}x^2 - 4.65\text{E+05}x + 2.39\text{E+07}$	0.9998
2	0.5263	$y = 5.32\text{E-08}x^6 - 9.86\text{E-05}x^5 + 7.62\text{E-02}x^4 - 3.14\text{E+01}x^3 + 7.27\text{E+03}x^2 - 8.98\text{E+05}x + 4.62\text{E+07}$	0.9996
3	0.6249	$y = 5.27\text{E-08}x^6 - 9.77\text{E-05}x^5 + 7.54\text{E-02}x^4 - 3.11\text{E+01}x^3 + 7.20\text{E+03}x^2 - 8.90\text{E+05}x + 4.58\text{E+07}$	0.9995
4	0.6896	$y = 5.11\text{E-08}x^6 - 9.47\text{E-05}x^5 + 7.32\text{E-02}x^4 - 3.01\text{E+01}x^3 + 6.98\text{E+03}x^2 - 8.63\text{E+05}x + 4.44\text{E+07}$	0.9992
5	0.8474	$y = 6.09\text{E-08}x^6 - 1.13\text{E-04}x^5 + 8.73\text{E-02}x^4 - 3.60\text{E+01}x^3 + 8.34\text{E+03}x^2 - 1.03\text{E+06}x + 5.31\text{E+07}$	0.9991

Entry	DMSO mole fraction	Equation	R^2
6	0.1640	$y = -1.18\text{E-08}x^6 + 2.21\text{E-05}x^5 - 1.73\text{E-02}x^4 + 7.20\text{E+00}x^3 - 1.69\text{E+03}x^2 + 2.11\text{E+05}x - 1.10\text{E+07}$	0.9996
7	0.3704	$y = -3.91\text{E-08}x^6 + 7.35\text{E-05}x^5 - 5.75\text{E-02}x^4 + 2.40\text{E+01}x^3 - 5.62\text{E+03}x^2 + 7.04\text{E+05}x - 3.67\text{E+07}$	0.9994
8	0.5953	$y = -1.74\text{E-08}x^6 + 3.26\text{E-05}x^5 - 2.55\text{E-02}x^4 + 1.06\text{E+01}x^3 - 2.48\text{E+03}x^2 + 3.10\text{E+05}x - 1.61\text{E+07}$	0.9998
9	0.7463	$y = -1.27\text{E-08}x^6 + 2.39\text{E-05}x^5 - 1.87\text{E-02}x^4 + 7.80\text{E+00}x^3 - 1.83\text{E+03}x^2 + 2.29\text{E+05}x - 1.19\text{E+07}$	0.9998
10	0.9363	$y = -4.70\text{E-09}x^6 + 8.81\text{E-06}x^5 - 6.87\text{E-03}x^4 + 2.86\text{E+00}x^3 - 6.70\text{E+02}x^2 + 8.36\text{E+04}x - 4.35\text{E+06}$	0.9998

Regression statistics

Table S2.3. Regression statistics for S-**DR4a**, S-**DR4b** and S-**DR5** in different pure organic solvents.

S-**DR4a**	Coefficients	Standard Error	t Stat	P-value	Lower 95%	Upper 95%	Lower 95.0%	Upper 95.0%
Intercept	−15.7681	0.0501	−314.6635	1.1541E-49	−15.8709	−15.6653	−15.8709	−15.6653
Polarity variable	1.4812	0.0825	17.9532	1.5430E-16	1.3119	1.6504	1.3119	1.6504
Viscosity variable	0.0248	0.0020	12.5940	8.1499E-13	0.0207	0.0288	0.0207	0.0288

S-**DR4b**	Coefficients	Standard Error	t Stat	P-value	Lower 95%	Upper 95%	Lower 95.0%	Upper 95.0%
Intercept	−13.4965	0.0637	−211.9693	4.9303E-45	−13.6271	−13.3658	−13.6271	−13.3658
Polarity variable	1.2265	0.1048	11.7002	4.4178E-12	1.0114	1.4416	1.0114	1.4416
Viscosity variable	0.0252	0.0025	10.0762	1.2062E-10	0.0201	0.0303	0.0201	0.0303

S-**DR5**	Coefficients	Standard Error	t Stat	P-value	Lower 95%	Upper 95%	Lower 95.0%	S-DR**4b**
Intercept	−13.5919	0.0747	−181.9138	3.3841E-39	−13.7461	−13.4377	−13.7461	−13.4377
Polarity variable	1.4518	0.1418	10.2364	3.1086E-10	1.1591	1.7445	1.1591	1.7445
Viscosity variable	0.0384	0.0028	13.8840	5.7730E-13	0.0327	0.0441	0.0327	0.0441

Table S2.4. Regression statistics for S-**DR4a** and S-**DR4b** in different solvents and solvent mixtures.

S-**DR4a**	Coefficients	Standard Error	t Stat	P-value	Lower 95%	Upper 95%	Lower 95.0%	Upper 95.0%
Intercept	−15.6907	0.0887	−176.8184	8.8605E-73	−15.8688	−15.5125	−15.8688	−15.5125
Polarity variable	1.6273	0.1284	12.6756	2.1979E-17	1.3695	1.8850	1.3695	1.8850
Viscosity variable	0.0101	0.0011	9.4054	9.9952E-13	0.0079	0.0123	0.0079	0.0123
S-**DR4b**	Coefficients	Standard Error	t Stat	P-value	Lower 95%	Upper 95%	Lower 95.0%	Upper 95.0%
Intercept	−13.4097	0.0958	−139.9987	1.2838E-67	−13.6020	−13.2174	−13.6020	−13.2174
Polarity variable	1.3753	0.1386	9.9250	1.6665E-13	1.0971	1.6535	1.0971	1.6535
Viscosity variable	0.0089	0.0012	7.6972	4.3327E-10	0.0066	0.0113	0.0066	0.0113

Transient absorption spectra
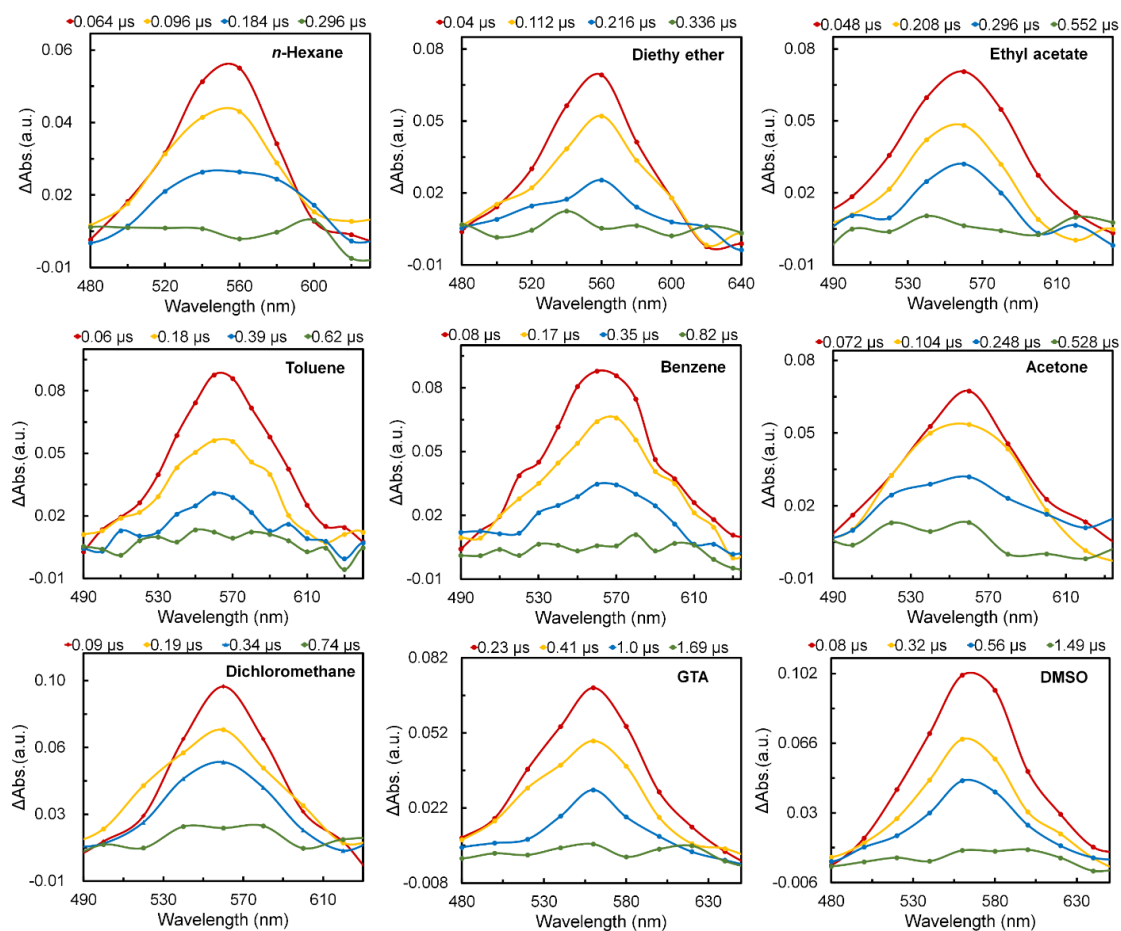
Figure S2.16. Sub-microsecond transient absorption spectra during the laser flash photolysis of **AZ4a** ($\lambda_{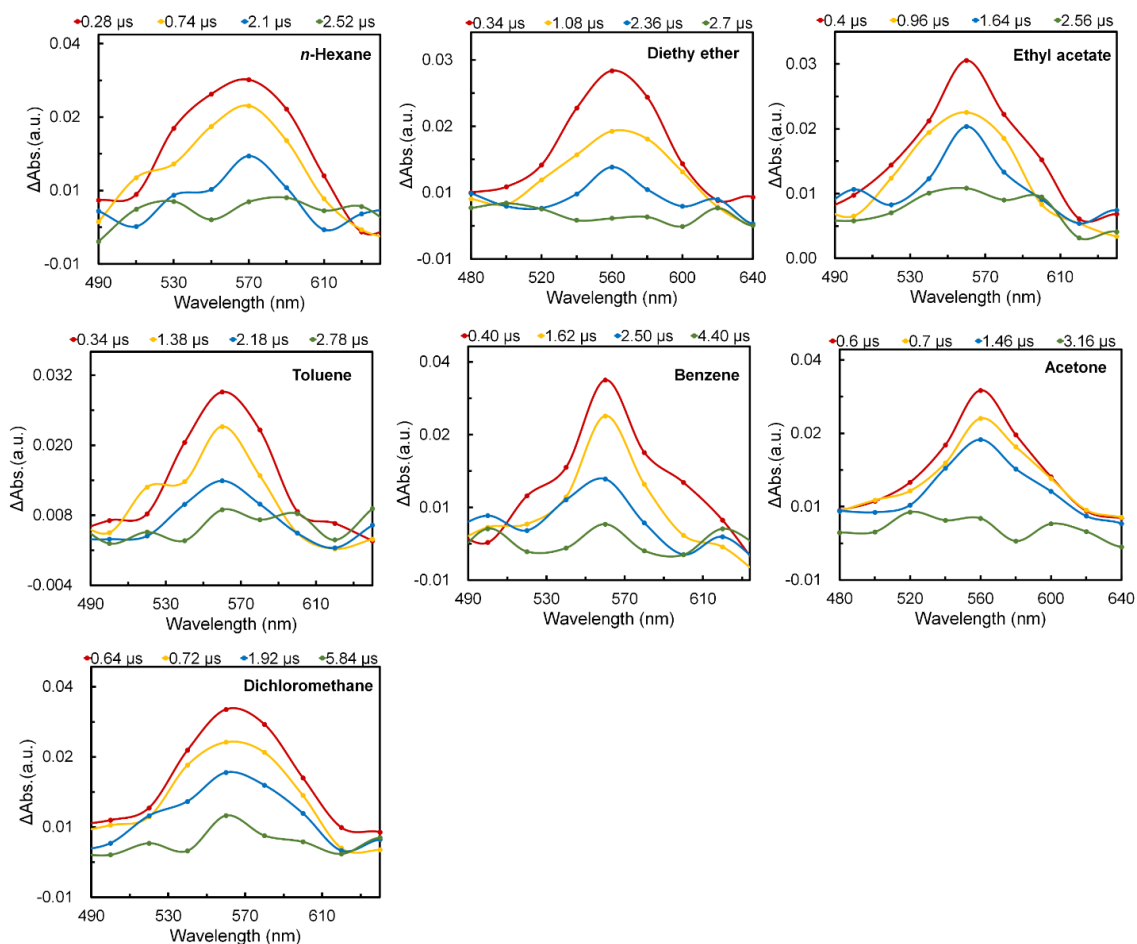emi}$ = 355 nm) at 293 K under a nitrogen in *n*-hexane, diethyl ether, ethyl acetate, toluene, benzene, acetone, dichloromethane, glycerin triacetin (GTA) and dimethyl sulfoxide (DMSO).
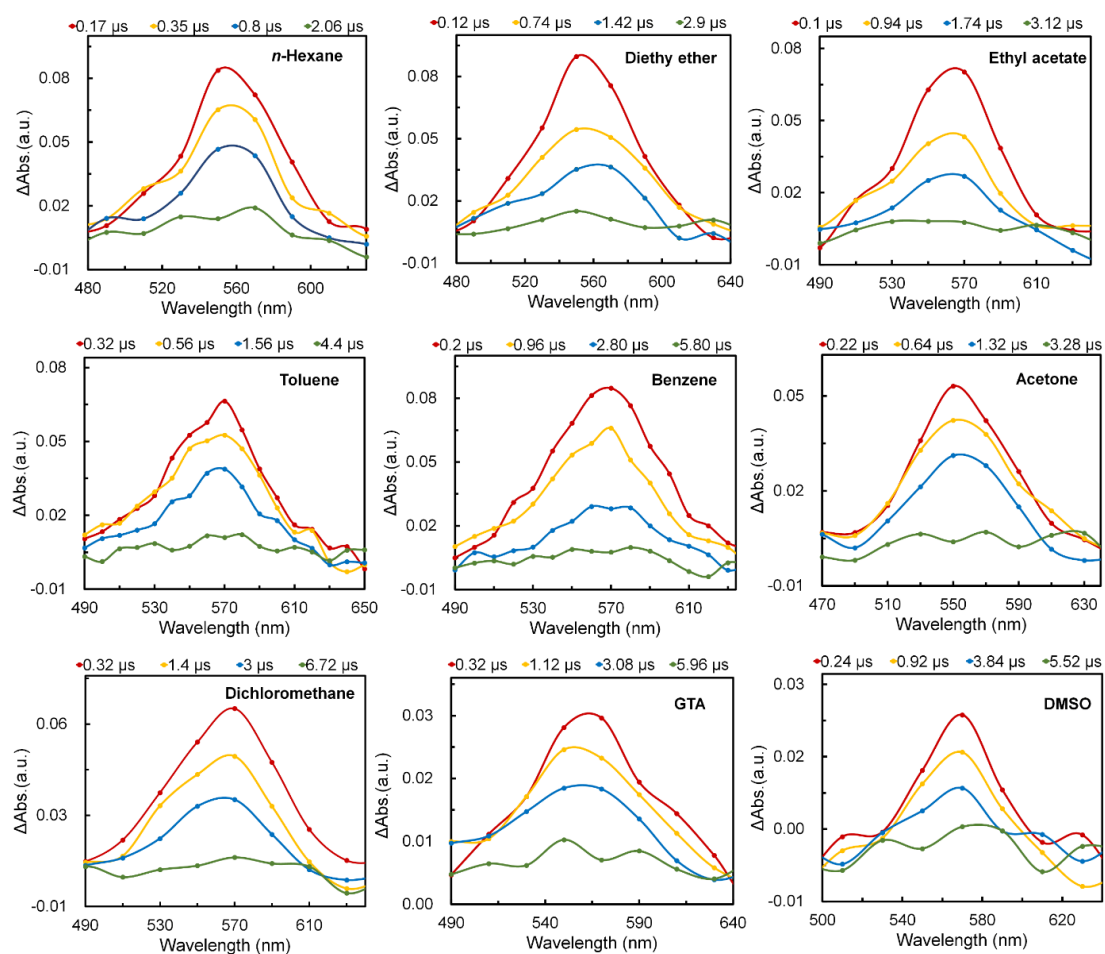
Figure S2.17. Sub-microsecond transient absorption spectra during the laser flash photolysis of **AZ4b** (λ_{emi} = 355 nm) at 293 K under a nitrogen in *n*-hexane, diethyl ether, ethyl acetate, toluene, benzene, acetone, dichloromethane, glycerin triacetin (GTA) and dimethyl sulfoxide (DMSO).
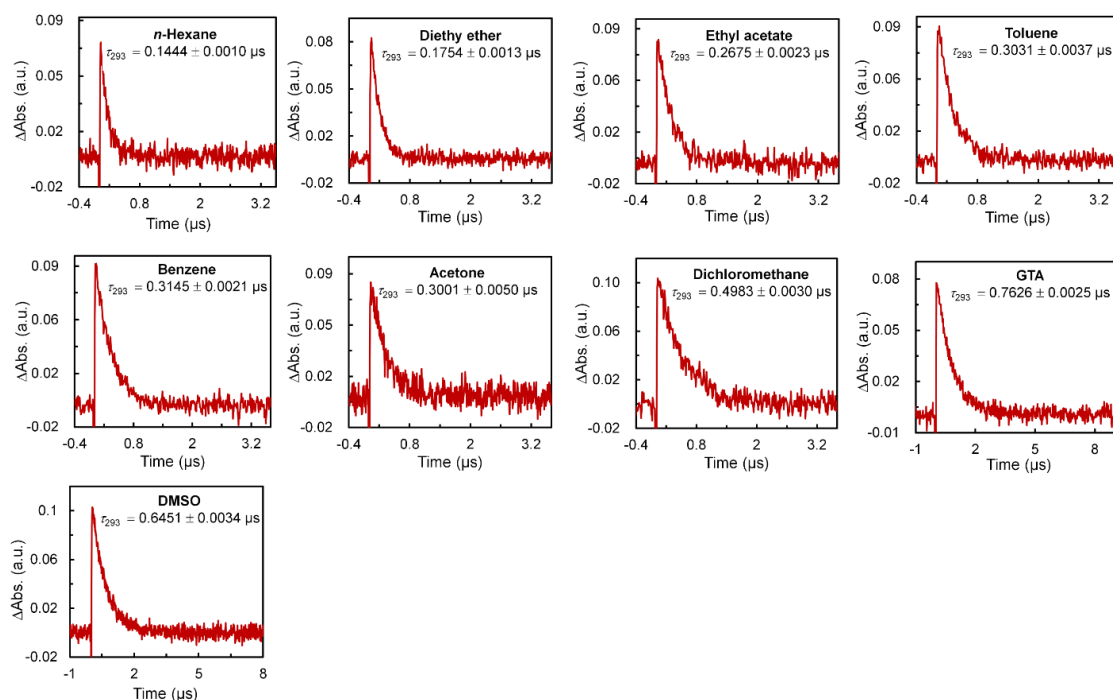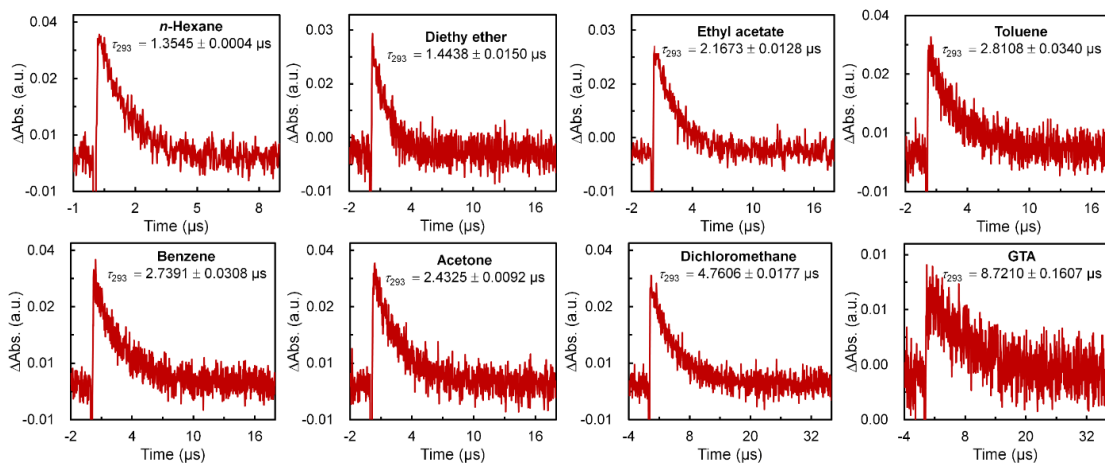
Figure S2.18. Time profiles at 560 nm of S-**DR4a** at 293 K under a nitrogen in *n*-hexane, diethyl ether, ethyl acetate, toluene, benzene, acetone, dichloromethane, glycerin triacetin (GTA) and dimethyl sulfoxide (DMSO). Lifetime are calculated from single-exponential decay model fitting.
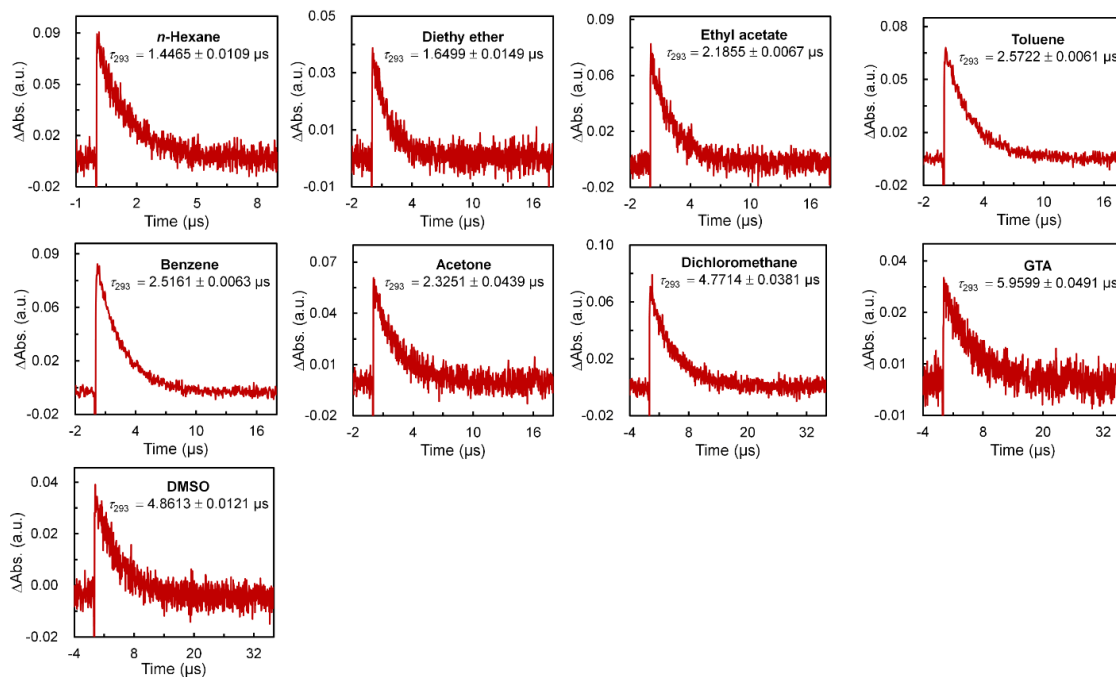
Figure S2.19. Time profiles at 570 nm of S-**DR4b** at 293 K under nitrogen in *n*-hexane, diethyl ether, ethyl acetate, toluene, benzene, acetone, dichloromethane, glycerin triacetin (GTA) and dimethyl sulfoxide (DMSO). Lifetime are calculated from single-exponential decay model fitting.

Figure S2.20. Sub-microsecond transient absorption spectra during the laser flash photolysis of **AZ5** (λ_{emi} = 355 nm) at 293 K under a nitrogen in *n*-hexane, diethyl ether, ethyl acetate, toluene, benzene, acetone and dichloromethane.

Figure S2.21. Time profiles at 560 nm of S-**DR5** at 293 K under nitrogen in *n*-hexane, diethyl ether, ethyl acetate, toluene, benzene, acetone, dichloromethane and glycerin triacetin (GTA). Lifetime are calculated from single-exponential decay model fitting.
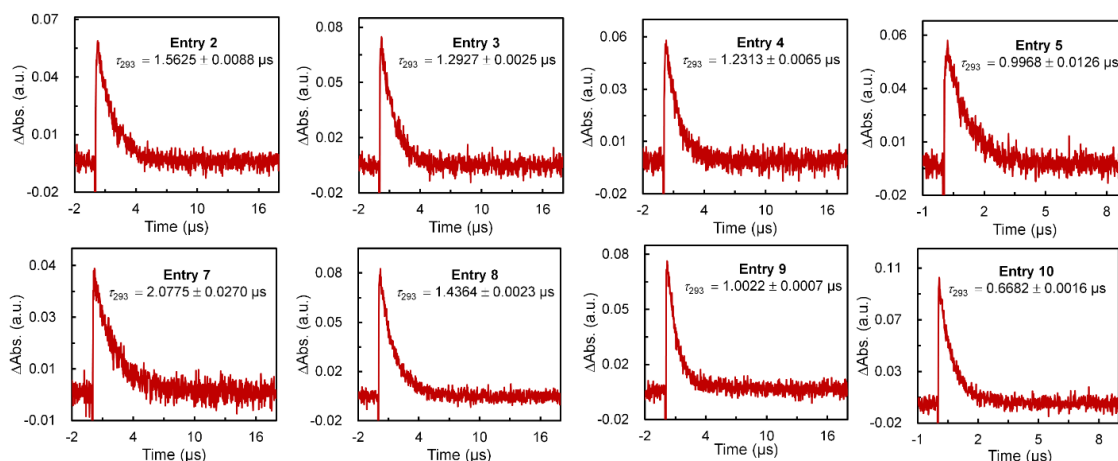
Figure S2.22. Time profiles at 560 nm of S-**DR4a** at 293 K under a nitrogen in binary systems containing [BMIM][PF$_6$] and GTA/DMSO (Table S2.1: entries 2−5 and 7−10). Lifetime are calculated from single-exponential decay model fitting.
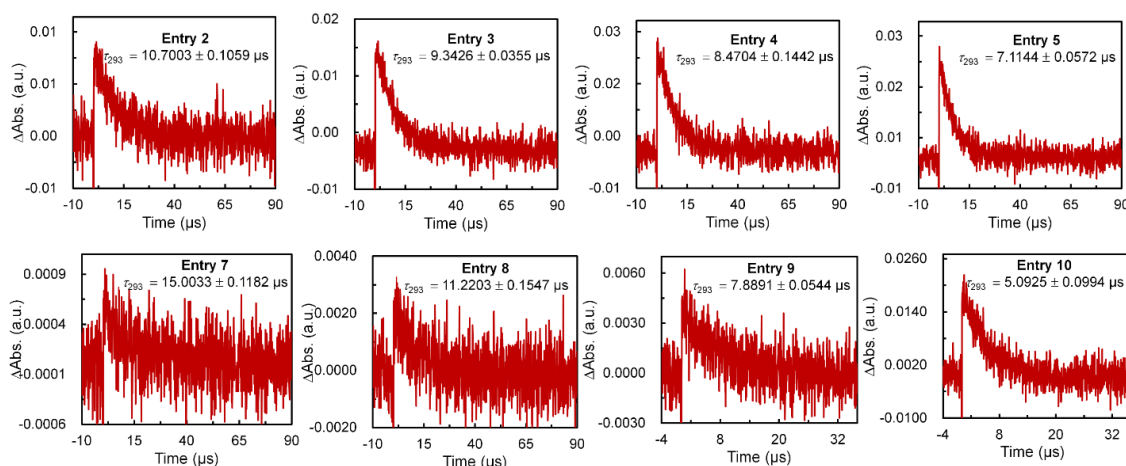
Figure S2.23. Time profiles at 570 nm of S-**DR4b** at 293 K under a nitrogen in binary systems containing [BMIM][PF$_6$] and GTA/DMSO (Table S2.1: entries 2−5 and 7−10). Lifetime are calculated from single-exponential decay model fitting.

Reference

(1) Abe, M.; Adam, W.; Heidenfelder, T.; Nau, W. M.; Zhang, X. Intramolecular and Intermolecular Reactivity of Localized Singlet Diradicals: The Exceedingly Long-Lived 2,2-Diethoxy-1,3-Diphenylcyclopentane-1,3-Diyl. *J. Am. Chem. Soc.* **2000**, *122*, 2019–2026.

(2) Abe, M.; Tada, S.; Mizuno, T.; Yamasaki, K. Impact of Diradical Spin State (Singlet vs Triplet) and Structure (Puckered vs Planar) on the Photodenitrogenation Stereoselectivity of 2,3-Diazabicyclo[2.2.1]Heptanes. *J. Phys. Chem. B* **2016**, *120*, 7217–7226.

(3) Nakagaki, T.; Sakai, T.; Mizuta, T.; Fujiwara, Y.; Abe, M. Kinetic Stabilization and Reactivity of π Single-Bonded Species: Effect of the Alkoxy Group on the Lifetime of Singlet 2,2-Dialkoxy-1,3-Diphenyloctahydropentalene-1,3-Diyls. *Chem. -A Eur. J.* **2013**, *19*, 10395–10404.

(4) Abe, M. Diradicals. *Chem. Rev.* **2013**, *113*. 7011–7088.

(5) Gulam, R. M.; Takahashi, T.; Ohga, Y. Dynamic Solvent Effects on the Thermal Isomerization of Zinc Dithizonate. *Phys. Chem. Chem. Phys.*, **2009**, *11*, 5170−5174

(6) Asano, T.; Matsuo, K.; Sumi, H. Effects of Solvent Fluctuations on the Rate of the Thermal *Z/E* Isomerization of *N*-Benzylideneanilines in a Highly Viscous Liquid Hydrocarbon. *Bull. Chem. Soc. Jpn.,* **1997**, *70*, 239–244.

(7) Quant, M.; Hamrin, A.; Lennartson, A.; Erhart, P.; Moth-Poulsen, K. Solvent Effects on the Absorption Profile, Kinetic Stability, and Photoisomerization Process of the Norbornadiene–Quadricyclanes System. *J. Phys. Chem. C* **2019**, *123*, 7081−7087.

(8) Rothenberger, G.; Negus, D. K.; Hochstrasser, R. M. Solvent Influence on Photoisomerization Dynamics. *J. Chem. Phys.* **1983**, *79*, 5360−5367.

(9) Bortolus, Pietro.; Monti, Sandra. Cis-Trans Photoisomerization of Azobenzene. Solvent and Triplet Donors Effects. *J. Phys. Chem.* **1979**, *83*, 648−652.

(10) Horbury, M. D.; Quan, W.-D.; Flourat, A. L.; Allais, F.; Stavros, V. G. Elucidating Nuclear Motions in a Plant Sunscreen during Photoisomerization through Solvent Viscosity Effects. *Phys. Chem. Chem. Phys.*, **2017**, *19*, 21127−21131.

(11) Quick, M. T.; Quick, M.; Ioffe, I. N.; Richter, C.; Mahrwald, R.; Druzhinin, S.; Kovalenko, S. A. Transient Rotamerism and Photoisomerization Dynamics of *Trans*- and *Cis*-Naphthylstilbene. *J. Phys. Chem. B* **2020**, *124*, 1049−1064.

(12) Onganer, Y.; Yin, M.; Bessire, D. R.; Quitevis, E. L. Dynamical Solvation Effects on the Cis-Trans Isomerization Reaction: Photoisomerization of Merocyanine 540 in Polar Solvents. *J. Phys. Chem.* **1993**, *97*, 2344–2354.

(13) Asano, T.; Okada, T. Thermal *Z–E* Isomerization of Azobenzenes. The Pressure, Solvent, and Substituent Effects. *J. Org. Chem.* **1984**, *49*, 4387−4391.

(14) Rice, J. K.; Baronavski, A. P. Ultrafast Studies of Solvent Effects in the Isomerization of Cis-Stilbene. *J. Phys. Chem.* **1992**, *96*, 3359–3366.

(15) Reichardt, C. *Solvents and Solvent Effects in Organic Chemistry*, Wiley, 2003.

(16) Asano, T.; Furuta, H.; Sumi, H. Two-Step Mechanism in Single-Step Isomerizations. Kinetics in a Highly Viscous Liquid Phase. *J. Am. Chem. Soc.* **1994**, *116*, 5545−5550.

(17) Zeglinski, D. M.; Waldeck, D. H. Evidence for Dynamic Solvent Effects on the Photoisomerization of 4,4'-Dimethoxystilbene. *J. Phys. Chem.* **1988**, *92*, 692−701.

(18) Hicks, J. M.; Vandersall, M. T.; Sitzmann, E. V.; Eisenthal, K. B. Polarity-Dependent Barriers and the Photoisomerization Dynamics of Molecules in Solution. *Chem. Phys. Lett.* **1987**, *135*, 413−420.

(19) Waldeck, D. H. Photoisomerization Dynamics of Stilbenes. *Chem. Rev.* **1991**, *91*, 415–436.

(20) Nikowa, L.; Schwarzer, D.; Troe, J.; Schroeder, J. Viscosity and Solvent Dependence of Low-barrier Processes:

Photoisomerization of *Cis* -stilbene in Compressed Liquid Solvents. *J. Chem. Phys.* **1992**, *97*, 4827–4835.

(21) Gegiou, D.; Muszkat, K. A.; Fischer, E. Temperature Dependence of Photoisomerization. VI. Viscosity Effect. *J. Am. Chem. Soc.* **1968**, *90*, 12–18.

(22) Saltiel, J.; D'Agostino, J. T. Separation of Viscosity and Temperature Effects on the Singlet Pathway to Stilbene Photoisomerization. *J. Am. Chem. Soc.* **1972**, *94*, 6445–6456.

(23) Goto, Y.; Takahashi, T.; Ohga, Y.; Asano, T.; Hildebrand, M.; Weinberg, N. Dynamic Solvent Effects on the Thermal Cyclization of a Hexadienone Formed from a Diphenylnaphthopyran: An Example of a System with Distinctly Separate Medium and Chemical Contributions to the Overall Reaction Coordinate. *Phys. Chem. Chem. Phys.*, **2003**, *5*, 1825–1830.

(24) Kitaoka, S.; Nobuoka, K.; Miura, J.; Ohga, Y.; Ishikawa, Y. First Observation for Dynamic Solvent Effect in Ionic Liquids. *Chem. Lett.* **2016**, *45*, 385–387.

(25) Goto, Y.; Sugita, K.; Takahashi, T.; Ohga, Y.; Asano, T. An Experimental Attempt to Identify a Moving Molecular Moiety in a Solvent Matrix. *Chem. Lett.* **2003**, *32*, 618–619.

(26) Sugita, K.; Goto, Y.; Ono, M.; Yamashita, K.; Hayase, K.; Takahashi, T.; Ohga, Y.; Asano, T. A New Application of High-Viscosity Kinetics. An Attempt to Identify a Site of Solvent Reorganizations around a Reactant. *Bull. Chem. Soc. Jpn.,* **2004**, *77*, 1803–1806.

(27) Asano, T. Kinetics in Highly Viscous Solutions: Dynamic Solvent Effects in "slow" Reactions. *Pure Appl. Chem.* **1999**, *71*, 1691–1704.

(28) Hitoshi Sumi. Theory on Reaction Rates in Nonthermallzed Steady States during Conformational Fluctuations in Viscous Solvents. *J. Phys. Chem.* **1991**, *95*, 3334–3350.

(29) Asano, T.; Cosstick, K.; Furuta, H.; Matsuo, K.; Sumi, H. Effects of Solvent Fluctuations on the Rate of Thermal *Z/E* Isomerization

of Azobenzenes and *N*-Benzylideneanilines. *Bull. Chem. So.c Jpn.,* **1996**, *69*, 551–560.

(30) Asano, T.; Matsuo, K.; Sumi, H. Effects of Solvent Fluctuations on the Rate of the Thermal *Z/E* Isomerization of *N*-Benzylideneanilines in a Highly Viscous Liquid Hydrocarbon. *Bull. Chem. So.c Jpn.,* **1997**, *70*, 239–244.

(31) Akisaka, R.; Ohga, Y.; Abe, M. Dynamic Solvent Effects in Radical–Radical Coupling Reactions: An Almost Bottleable Localised Singlet Diradical. *Phys*. *Chem*. *Chem*. *Phys*., **2020**, *22*, 27949–27954

(32) Wang, Z.; Akisaka, R.; Yabumoto, S.; Nakagawa, T.; Hatano, S.; Abe, M. Impact of the Macrocyclic Structure and Dynamic Solvent Effect on the Reactivity of a Localised Singlet Diradicaloid with π-Single Bonding Character. *Chem. Sci.,* **2021**, *12*, 613–625.

(33) Hatano, M.; Sakamoto, T.; Mizuno, T.; Goto, Y.; Ishihara, K. Chiral Supramolecular U-Shaped Catalysts Induce the Multiselective Diels–Alder Reaction of Propargyl Aldehyde. *J. Am. Chem. Soc.* **2018**, *140*, 16253–16263.

(34) Ye, J.; Fujiwara, Y.; Abe, M. Substituent Effect on the Energy Barrier for σ-Bond Formation from π-Single-Bonded Species, Singlet 2,2-Dialkoxycyclopentane-1,3-Diyls. *Beilstein J. Org. Chem.* **2013**, *9*. 925–933.

(35) Abe, M.; Adam, W.; Hara, M.; Hattori, M.; Majima, T.; Nojima, M.; Tachibana, K.; Tojo, S. On the Electronic Character of Localized Singlet 2,2-Dimethoxycyclopentane-1,3-Diyl Diradicals: Substituent Effects on the Lifetime. *J. Am. Chem. Soc.* **2002**, *124*, 6540–6541.

(36) Hoga, H. E.; Olivieri, G. V.; Torres, R. B. Experimental Measurements of Volumetric and Acoustic Properties of Binary Mixtures of 1-Butyl-3-Methylimidazolium Hexafluorophosphate with Molecular Solvents. *J. Chem. Eng. Data* **2020**, *65*, 3406–3419.

(37) Zafarani-Moattar, M. T.; Majdan-Cegincara, R. Viscosity, Density,

Speed of Sound, and Refractive Index of Binary Mixtures of Organic Solvent + Ionic Liquid, 1-Butyl-3-Methylimidazolium Hexafluorophosphate at 298.15 K. *J. Chem. Eng. Data* **2007**, *52*, 2359–2364.

(38) Reichardt, C. Solvatochromic Dyes as Solvent Polarity Indicators. *Chem. Rev.* **1994**, *94*, 2319–2358.

(39) Spange, S.; Lungwitz, R.; Schade, A. Correlation of Molecular Structure and Polarity of Ionic Liquids. *J. Mol. Liq.,* **2014**, *192*, 137–143.

(40) Carda–Broch, S.; Berthod, A.; Armstrong, D. W. Solvent Properties of the 1-Butyl-3-Methylimidazolium Hexafluorophosphate Ionic Liquid. *Anal. Bioanal. Chem* **2003**, *375*, 191–199.

Chapter 3.
Summary and Outlook

Localized singlet diradicals, as key intermediates in the homolytic bond cleavage and formation reactions, have attracted significant attention in their structures, reactivity and kinetic stabilization. Studies of substituent effects have proved a fact that the localized singlet diradicals were expected to be generated from the photodenitrogenation of corresponding azoalkanes with a strong absorption at around 570 nm when electron-withdrawing groups such as F or OR locate in C2 position. Defined as having π-single bonding character with very small HOMO-LUMO energy gap, localized singlet diradicals take place fast radical-radicals coupling reaction generally. The lifetimes of localized singlet diradicals that determined by the rate constant of radical-radical coupling reaction can be extended effectively by useful strategies such as the electronic hyperconjugation of terminal p-MeO of the phenyl rings, steric effect induced by the bulky substituent and the dramatically stretch effect arising from the macrocycle ring. Zwitterionic resonance structures is a characteristic feature found in localized singlet diradicals that afford the reaction of diradicals strongly affected by the solvent polarity. Dynamic solvent effect especially in high-viscous solvent where the transition state theory is invalidated plays a significant role in the reaction of localized single diradicals. Given previously studies on the isomerization in solvent, the isomerization rate was sensitive to the solvent polarity and viscosity. Besides, viscosity could also be used as a useful tool to explore the molecular motion during the isomerization process.

In present thesis, dynamic solvent effect has been elucidated on the lifetime of localized singlet 2,2-alkoxy-1,3-diyl diradicals S-**DR4a**, S-**DR4b** and S-**DR5** with π-single bonding thoroughly in 18 solvents including the binary solvents combined with ionic liquid and organic solvent. The experimental results showed that lifetime of diradicals increased with an increase in solvent polarity and viscosity. Specially, in low viscosity solvent ($\eta < 1$ mPa s), lifetime substantially dependents on polarity. Slower radical-radical coupling reaction was observed in more polar solvents. In high viscous solvents ($2 < \eta < 126$ mPa s), lifetime was largely affected by viscosity while the polarity

effect was also nonnegligible. Furthermore, regression analysis was performed to evaluate the polarity and viscosity effect on lifetime of diradicals and confirm the difference of sensitivity for polarity and viscosity for S-**DR4a**, S-**DR4b** and S-**DR5**. Comparison of S-**DR4b**, S-**DR5** with long carbon chain at remote position from the reaction site has more pronounce viscosity effect which revealed the relative motion of cyclopentane moiety during the isomerization from the planar single diradicals to ring-closing compounds featuring puckered structure.

The present study provides insight into the nature of singlet diradicals, in particular, understanding π-single bonding and zwitterionic characters. Moreover, the study furnishes a demonstrative example that dynamic solvent effects served as a promising strategy to shed a light on the mechanism of isomerization in solvents. Much efforts are underway to investigate the design of longer lifetime singlet diradicals and the reactivity of diradicals and multiradicals.

Acknowledgement

(CSC) for my Ph.D. scholarship. Meanwhile, as an overseas student in Japan, I really appreciate all the friendly help from the Japanese to me!

<div align="right">August 2022   LIU QIAN</div>

List of Publication

Impacts of Solvent and Alkyl Chain Length on the Lifetime of Singlet
Cyclopentane-1,3-diyl Diradicaloids with π-Single Bonding

Qian Liu, Zhe Wang, Manabu Abe